


Analysis Report
Task 5 of AP-088
Evaluation of Mining Scenarios

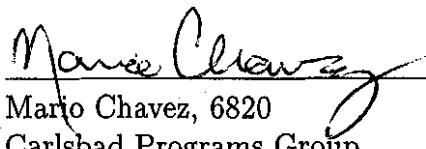
(AP-088: Analysis Plan for Evaluation of the Effects of
Head Changes on Calibration of Culebra Transmissivity Fields)

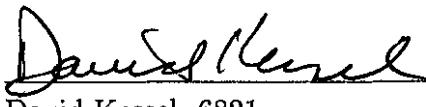
Task Number 1.4.1.1, ERMS #531138

Report Date: October 8, 2003

Author: 
Thomas S. Lowry, 6115
Geohydrology Department
Date: 10/8/03

Technical Review: 
Sean A. McKenna, 6115
Geohydrology Department
Date: 10/8/03

QA Review: 
Mario Chavez, 6820
Carlsbad Programs Group
Date: 10/17/03

Management Review: 
David Kessel, 6821
Manager, Performance Assessment
and Decision Analysis
Date: 10/17/03

WIPP:1.4.1.1:TD:QA-L:DPRP1:522085

INFORMATION ONLY

Contents

Table of Contents	2
List of Figures	4
List of Tables	6
1 Introduction	7
1.1 Background	7
1.2 Purpose	7
1.3 Outline	8
2 Approach	9
2.1 Overview	9
2.2 Software	10
2.3 File Naming Convention	12
2.4 Model Domain and Discretization	14
2.5 Boundary and Initial Conditions	17
2.6 Subtask 1: Determination of Potential Mining Areas	23
2.7 Subtask 2: Use of Mining Zones in Forward Simulations	26
2.8 Subtask 3: Particle Tracking using DTRKMF	27
3 Modeling Assumptions	27
4 Results	28
4.1 Particle Travel Times	28
4.2 Travel Direction	32
4.3 Extreme Values	37
5 Summary	46
Appendices:	50
A. Source Code for FM.F	50
B. Source Code for PM.F	53

C. Source Code for REFINE.F	56
D. Source Code for BA.F	58
E. Source Code for PTOUT.F	60
F. Source Code for PTPLOT.F	62
G. Script Code for MINING.SH	64
H. Script Code for POST.SH	66
I. Script Code for POST-FLOW.SH	67
J. Qualified runs and random mining factors	68

List of Figures

1	Software and information flow-chart. Elements within the dashed box are part of AP-100.	13
2	Directory tree of Task 5 files and programs. <i>Note that the subdirectories d01r02 and d01r04 appearing under the R*/full and R*/partial directories represent the first two of 100 subdirectories.</i>	15
3	Modeling domain and boundary conditions for the CRA grid configuration. The western no-flow boundary coincides with the groundwater divide underneath Nash draw.	18
4	1996 modeling domain and outline of full-mining zones (red) overlaid on current full-mining zones and modeling domain.	19
5	1996 modeling domain and outline of partial-mining zones (red) overlaid on current partial-mining zones and modeling domain.	20
6	Initial heads across modeling domain.	22
7	Potential potash distribution in regional area.	24
8	Potential potash distribution within WIPP boundary (red). The repository structure is shown in the center. Coordinates are UTM NAD 27.	25
9	Cumulative distribution function plot of the full-, partial-, and non-mining scenarios for the CRA.	29
10	Normalized pore velocities for the full-mining case. Red indicates zones of high velocity. The black outline shows the full-mining zones and the red box is the WIPP LWB. The T-field used to produce the velocity profile is averaged across all T-field/replicate combinations for the full-mining scenario (300 T-fields in total).	30
11	Cumulative distribution function plot of the 3 full-mining scenario replicates as compared to the CCA full-mining scenario. An increase in travel time can be seen for the CRA scenarios.	32
12	Cumulative distribution function plot of the 3 partial-mining scenario replicates as compared to the CCA partial-mining scenario. An increase in travel time can be seen for the CRA scenarios.	33
13	Particle tracks for replicate 1 for the full-mining scenario.	34
14	Particle tracks for replicate 2 for the full-mining scenario.	34
15	Particle tracks for replicate 3 for the full-mining scenario.	35

16	Particle tracks for replicate 1 for the partial-mining scenario. .	35
17	Particle tracks for replicate 2 for the partial-mining scenario. .	36
18	Particle tracks for replicate 3 for the partial-mining scenario. .	36
19	Correlation between the random mining factor and Log-travel time.	38
20	Head contours and particle track for the maximum travel time T-field (d04r01-R2) for the full-mining case. The WIPP bound- ary is the red box in the center of the figure and the particle track is the blue track originating from the approximate center of the WIPP.	40
21	Head contours and particle track for the minimum travel time T-field (d01r07-R2) for the full-mining case. The WIPP bound- ary is the red box in the center of the figure and the particle track is the blue track originating from the approximate center of the WIPP.	41
22	Head contours and particle track for the median travel time T- field (d10r09-R1) for the full-mining case. The WIPP bound- ary is the red box in the center of the figure and the particle track is the blue track originating from the approximate center of the WIPP.	42
23	Head contours and particle track for the maximum travel time T-field (d04r01-R2) for the partial-mining case. The WIPP boundary is the red box in the center of the figure and the particle track is the blue track originating from the approxi- mate center of the WIPP.	43
24	Head contours and particle track for the minimum travel time T-field (d08r01-R3) for the partial-mining case. The WIPP boundary is the red box in the center of the figure and the particle track is the blue track originating from the approxi- mate center of the WIPP.	44
25	Head contours and particle track for the median travel time T-field (d01r04-R1) for the partial-mining case. The WIPP boundary is the red box in the center of the figure and the particle track is the blue track originating from the approxi- mate center of the WIPP.	45

NO MULTIMEDIA

INFORMATION ONLY

List of Tables

1	Modeling software for Task 5.	11
2	Input and output files used for Task 5. File names in <i>italics</i> denote files associated with Tasks 2 and 3 of AP-100.	16
3	The coordinates of the corners of the numerical model domain in UTM NAD27 Coordinates.	21
4	The coordinates of the corners of the WIPP land withdrawal boundary (LWB) in UTM NAD27 Coordinates.	21
5	Travel time statistics in years for the full and partial mining scenarios as compared to the non-mining scenario from Task 4.	31

1 Introduction

This analysis report describes the activities of Task 5 of AP-088, "Analysis Plan for Evaluation of the Effects of Head Changes on Calibration of Culebra Transmissivity Fields" (Beauheim, 2002). The purpose of this Task is to evaluate the effects of future potash mining on flow and transport in the Culebra.

1.1 Background

The Waste Isolation Pilot Plant (WIPP) is located in southeastern New Mexico and has been developed by the U.S. Department of Energy (DOE) for the geologic (deep underground) disposal of transuranic (TRU) waste. Containment of TRU waste at the WIPP is regulated by the U.S. Environmental Protection Agency (EPA) according to the regulations set forth in Title 40 of the Code of Federal Regulations, Parts 191 and 194. The DOE demonstrates compliance with the containment requirements in the regulations by means of a performance assessment (PA), which estimates releases from the repository for the regulatory period of 10,000 years after closure.

In October 1996, DOE submitted the Compliance Certification Application (CCA) to the EPA, which included the results of extensive PA analysis and modeling. After an extensive review, in May 1998 the EPA certified that the WIPP met the criteria in the regulations and was approved for disposal of transuranic waste. The first shipment of waste arrived at the site in March 1999.

The results of the PA conducted for the CCA were subsequently summarized in a Sandia National Laboratories (SNL) report (Helton et al., 1998) and in refereed journal articles (Helton and Marietta, 2000).

The DOE is required to submit an application for recertification every five years after the initial receipt of waste. The recertification applications take into account any information or conditions that have changed since the original certification decision. Accordingly, the DOE is conducting a new PA in support of the Compliance Recertification Application (CRA).

1.2 Purpose

Potash mining in the WIPP area involves resource extraction below the Culebra dolomite in the underlying McNutt Potash zone, which is part of the

larger Salado Formation (Ramsey et al., 1996). It is hypothesized that subsidence of the Culebra due to mining extraction causes fracturing and unconsolidation of the aquifer material that results in higher transmissivities. This increase in transmissivity may significantly change the regional groundwater flow pattern in the Culebra and additionally the transport of any nuclides entering the aquifer from the underlying repository. The purpose of this analysis is to determine the impact of the increase in transmissivity in the Culebra due to mining on groundwater flow direction and velocity. Specifically, this task involves three subtasks:

1. Update from previous versions (Ramsey et al., 1996; Wallace, 1996), the potential areas of future potash mining that are within the model domain and map those areas to the new computational grid
2. Modify the calibrated transmissivity fields (T-fields) from Task 4 of AP-088 and Task 1 of AP-100 to include mining effects and run steady-state groundwater flow simulations to calculate the new flow-field
3. Perform particle tracking using the new mining-affected flow-fields to determine travel times to the WIPP land-withdrawal boundary (LWB)

This analysis report highlights the differences and additions relative to the "Analysis Package for the Culebra Flow and Transport Calculations (Task 3) of the Performance Assessment Analysis Supporting the Compliance Certification Application" (Ramsey et al., 1996) and the "Summary Memo of Record for NS-11; Subsidence Associated with Mining Inside or Outside the Controlled Area" (Wallace, 1996) that was required by the EPA pursuant to 40CFR Part 194, which contains the minimum specifications for incorporating potash-mining impacts upon the performance of the WIPP repository. The Summary Memo of Record for NS-11 is the documentation of the efforts to meet regulation 40CFR Part 194 as part of the 1996 certification of the WIPP. The reader is encouraged to review those documents for background information.

1.3 Outline

This report documents the data, methods and summary results of the work done as Task 5 of Analysis Plan 088 (Beauheim, 2002). The sections of this report and a brief description of each subsection are:

Section 2: Approach

- 2.1: Overview;** Provides an overview and summary of the modeling approach.
- 2.2: Software;** Describes the software usage and information flow between programs.
- 2.3: File Naming Convention;** Describes the file naming conventions and the input and output files for each program.
- 2.4: Modeling Domain and Discretization;** Outlines the computational grid and modeling domain in terms of regional scale coordinates.
- 2.5: Boundary and Initial Conditions;** Describes the determination and justification for the boundary and initial modeling conditions.
- 2.6: Determination of Potential Mining Areas;** Describes the methodology of determining the potential mining areas.
- 2.7: Use of Mining Zones in Forward Simulations;** Describes how mining zones are applied to the flow model.
- 2.8: Particle Tracking using DTRKMF;** Describes the use of the **DTRKMF** particle tracking code.

Section 3: Modeling Assumptions

Summarizes the major assumptions of Task 5.

Section 4: Results

Presents results from the Task 5 mining scenario simulations.

Section 5: Summary

Presents a summary of this entire report.

2 Approach

2.1 Overview

This analysis investigates two mining-altered scenarios. The first includes mining in all potential mining zones both inside and outside the land withdrawal boundary and is called the full-mining scenario. The second includes only the potential mining zones outside the LWB and is called the partial-mining scenario. The impacts are considered by scaling each calibrated T-field generated from Task 4 of AP-088 (McKenna and Hart, 2003b) and selected by Task 1 of AP-100 (Beauheim, 2003) in regions deemed to contain

economically-extractable potash resources by a random factor between 1 and 1000. The range of this factor is set by the EPA in regulation 40CFR Part 194, p. 5229 (Federal Register/vol. 61, No. 28) and is reproduced in Wallace (1996). The scaling factor for each T-field is provided from Latin Hypercube Sampling (LHS).

A forward steady-state flow model is run for each new T-field under each mining scenario (full and partial), for three replicates of mining factors, resulting in 600 simulations (there are 100 qualified T-fields passed from Task 1 of AP-100, see Beauheim (2003)). Particle tracking is performed on the modified flow fields to determine the flow path and groundwater travel time from a point above the center of the WIPP disposal panels to the LWB. A cumulative probability distribution function (CDF) is produced for each mining scenario (as well as an undisturbed scenario generated from Task 4 of AP-088) that describes the probability of a conservative tracer reaching the LWB at a given time. Incorporated into the Task described here (Task 5, AP-088), are Tasks 2 and 3 of AP-100 (Leigh et al., 2003) that refine the modeling grid used here (Task 2) and generates a forward steady-state flow field on the refined grid (Task 3). The detailed steps involved in Tasks 2 and 3 of AP-100 can be found in Lowry (2003). Their inclusion in this report is only to provide context to the procedures and approach of Task 5.

2.2 Software

The forward steady-state flow modeling is performed using **MODFLOW 2000 (MF2K)**, version 1.6 (Harbaugh et al., 2000). The same executable used for the Task 4 calibration is used in this analysis. **MF2K** is a modular, finite-difference code for solving the groundwater flow equation on a two- or three-dimensional rectilinear grid. The code **DTRKMF** (Rudeen, 2003) is used to perform the particle-tracking simulations. **DTRKMF** calculates particle tracks in 2-D or 3-D for steady-state and time-dependent, variably saturated flow fields. The particles are tracked cell-by-cell using a semi-analytical solution (WIPP_PA, 2003d). **DTRKMF** assumes that the velocities vary linearly between the cell faces as a function of the space coordinate and, for time-dependent cases, that the velocities at the faces vary linearly between time planes. It directly reads the cell-by-cell flow budget file from **MF2K** and uses those values to calculate the velocity field. The modeling codes for Task 5 are listed in Table (1).

Several FORTRAN utility codes are used for data conversion purposes.

Table 1: Modeling software for Task 5.

Code Name	Description	ERMS #
MODFLOW 2000 , v1.6	Groundwater Flow Model	523867
DTRKMF	Particle-tracking model	523244

These codes are **FM.F**, **PM.F**, **REFINE.F**, **BA.F**, **PTOUT.F**, and **PT-PLOT.F**. Their source codes are reproduced in the Appendices. The first, **FM.F** is the full-mining scenario pre-processor. This code reads in the calibrated T-fields passed from Task 1 of AP-100, as well as the random mining multiplicative factor, multiplies the transmissivity value in the cells that lie within the mining zone areas by the random factor, and then outputs the modified T-field to a file. Likewise, **PM.F** performs the same task but for the partial-mining scenario. **REFINE.F** is specific to Task 2 of AP-100 (Leigh et al., 2003) and converts the calibrated T-field from the 100x100 m uniform cell size (see below) that is used here, to a 50x50 m uniform cell size that is used for Task 6 of AP-100. Task 6 of AP-100 performs the radionuclide transport calculations in the mining-affected flow fields using **SECOTP2D**. The grid conversion is a simple conversion, meaning each grid cell from the 100x100 m cell-sized grid becomes four 50x50 m sized cells, each with the same attributes as the original 100x100 m cell. The attributes include transmissivity, top and bottom elevations, initial head, and the IBOUND array (the IBOUND array designates the active/inactive/constant-head status for each cell). Output from **REFINE.F** is formatted for input to **MF2K**, which is then run to provide the cell-by-cell flow budget file on the 50x50 m cell grid. This step is Task 3 of AP-100. Since **MF2K** is run on a qualified multiple processor Linux cluster (SNL Dept. 6115) and **SECOTP2D** is run on ES-40, ES-45, and/or 8400 Compaq ALPHA computers running Open VMS Version 7.3-1 (WIPP_PA, 2003a,b,c), the binary files are unable to be transferred directly between the two platforms. Thus, **BA.F** is used to read in the binary budget file from **MF2K** and write it out in ASCII format. The ASCII text file is then transferred to the ALPHA computers via FTP. The other two codes, **PTOUT.F** and **PTPLOT.F** are data manipulation codes and are used to convert the **DTRKMF** output to a format that is suitable for summary and visualization.

The Department of Defense Groundwater Modeling System (GMS, ver-

sion 4.0) software is used for digitizing the mining zone areas onto the computational grid as well as for general visualization purposes (GMS, 2003). **GMS** is a groundwater modeling and geo-statistical software package that provides a graphical user interface to numerous groundwater modeling codes. Its strength lies in the ability to apply spatially varying data (e.g. the mining zones) to a discrete grid of any given size. **GMS** is not used to perform any calculations or data conversions. Its use in this Task is to provide visual aid in matching the computational grid to the mining zone map and to perform a coordinate conversion for the mining zone map (see below).

In addition, several Linux shell scripts are used to help automate and coordinate running the programs. Specifically, they are **MINING.SH**, **POST.SH**, and **POST-FLOW.SH**. **MINING.SH** is the main script that coordinates the running of each model and the other scripts in succession. Starting with each replicate directory, **MINING.SH** creates separate directories for the full and partial-mining scenarios, and then under each of those directories, a separate directory for each T-field. The naming convention of the files and T-fields is addressed in Section 2.3. With the directories set-up, **MINING.SH** then calls **FM.F**, **PM.F**, and **REFINE.F** to produce the 100x100 m modified T-fields and the refined 50x50 m modified T-fields, **MF2K** to run the 100x100 m flow model, **DTRKMF** to perform the particle tracking, and then **MF2K** again to run the 50x50 m flow model. Finally **MINING.SH** calls **POST.SH** to gather all the **DTRKMF** output into a single directory called *ptout*, **PTOUT.F** to combine all the **DTRKMF** output into two files (one each for the full and partial-mining scenarios), **BA.F** to convert the binary 50x50 m budget file to ASCII format, and **POST-FLOW.SH** to gather the ASCII budget files into a single directory called *aff*. The shell scripts are reproduced in Appendices (G) to (I).

Figure (1) shows the software and information flow chart, with the output/input relationship between the different programs.

2.3 File Naming Convention

The file naming convention for this Task is kept consistent with that of Task 4 (McKenna and Hart, 2003b) to prevent confusion during comparisons. All calculations are performed on the 6115 Linux cluster and are done in a separate directory for each T-field. The general path for the T-field directories is:

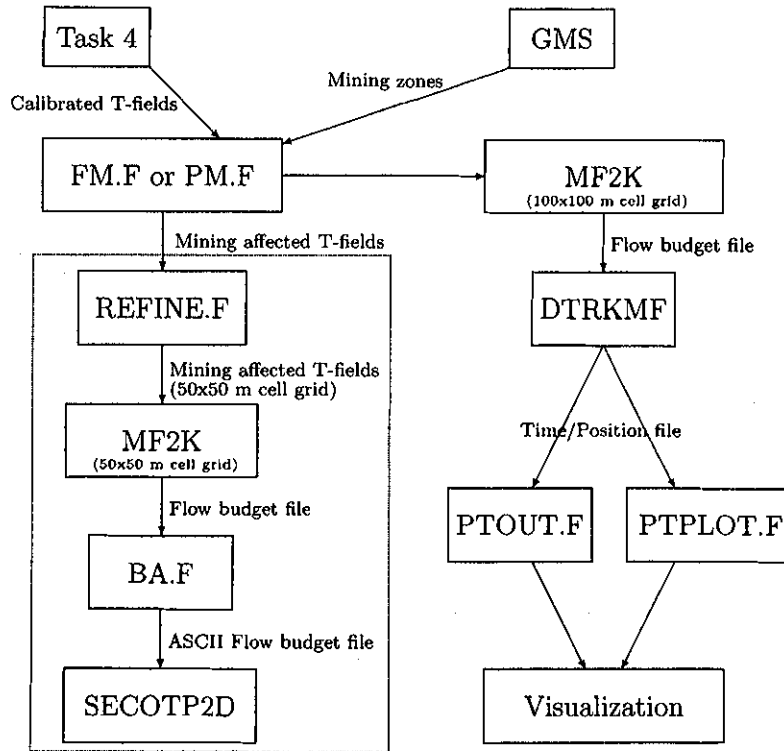


Figure 1: Software and information flow-chart. Elements within the dashed box are part of AP-100.

/home3/tslowry/wipp/mining/R/ [scenario]/d##r##*

where, R^* is either R1, R2, or R3, depending on the mining factor replicate, $[scenario]$ is either 'full' or 'partial', depending on the mining scenario, and $d##r##$ is the original base transmissivity field naming convention as described in Holt and Yarbrough (2003). The $##$'s next to 'd' ranges from 01 to 22 and next to the 'r' it ranges from 01 to 10. In Task 4 of AP-088, 150 calibration runs were attempted, with 137 able to be calibrated. However, some of the calibrated T-fields can be a poor representation of the known field so that qualifying criteria are used (Beauheim, 2003) to reduce the 137 calibrated fields to 100. Thus for the naming convention, not all values of $##$ will appear as a directory. In addition, there are two data di-

Y:\M0\WIPP\AP-088\Task 4

rectories ('100x100' and '50x50') that contain the **MF2K** and **DTRKMF** input files for the 100x100 m and 50x50 m cell grid, respectively, and two directories ('scripts' and 'source') that contain backups of the shell scripts and the FORTRAN source files for the files described above. These directories are subdirectories of */home3/tslowry/wipp/mining*. The parent copy of the shell scripts and the FORTRAN executables are kept in and run from */home3/tslowry/wipp/mining*. A schematic of the directory tree is shown in Figure (2). The input and output files that will remain archived in the directories are listed in Table (2).

2.4 Model Domain and Discretization

The model domain used in Task 5 is the same as that used in Task 4. The original intent for Task 4 was to use 50x50 m cells, but due to computational constraints in the calibration process it was decided that the grid should be coarsened to the 100x100 m uniform cell grid. This change is discussed fully in McKenna and Hart (2003b). For the **SECOTP2D** input, model parameters from the Task 4 grid are exactly delineated onto a 50x50 m cell grid meaning each 100x100 m cell is split into four 50x50 m cells. Each of the four smaller cells is assigned the same attribute as the original cell. While this is not a true refinement from a data resolution point of view, it does provide the needed compatibility to the 50x50 m **SECOTP2D** grid.

A general description of the modeling domain and grid-layout is given in McKenna and Hart (2003a) and is reproduced here for completeness:

The north-south and east-west extent of the model domain was specified by Richard Beauheim, Robert Holt, and Sean McKenna. This determination considered several factors including: 1) hydrogeological features in the vicinity of the WIPP site that could serve as groundwater flow boundaries (e.g. Nash Draw); 2) the areas to the north of the WIPP site that might create additional recharge to the Culebra due to water applied to potash tailings pile; and 3) the limits imposed on the domain size by the available computational resources and the desired fine scale discretization of the domain within the groundwater model. The final model domain is rectangular and aligned with the north-south and east-west directions. The coordinates of each corner of the domain are given in Table 1 in UTM (*NAD27*) coordinates. A no-flow

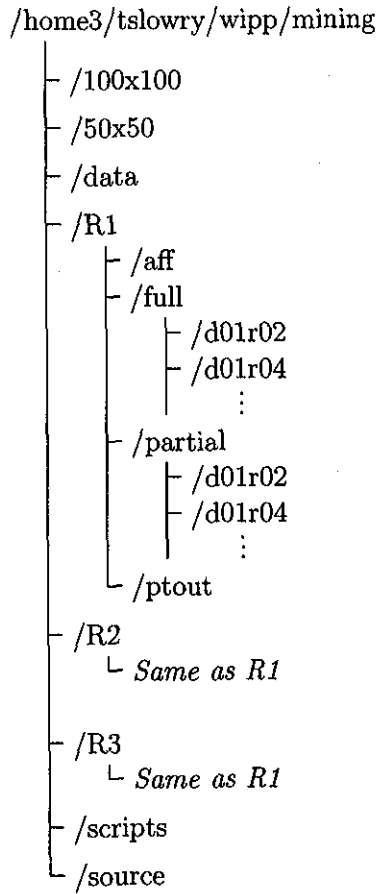


Figure 2: Directory tree of Task 5 files and programs. Note that the subdirectories *d01r02* and *d01r04* appearing under the *R*/full* and *R*/partial* directories represent the first two of 100 subdirectories.

Table 2: Input and output files used for Task 5. File names in *italics* denote files associated with Tasks 2 and 3 of AP-100.

Directory	File	Description
/mining	Good_runs.txt	List of good T-fields in d##r### format
	mFR*.txt	Mining factors (R* = R1, R2, or R3)
	Replicate.txt	Replicate number input file
	Full_mining.dat	Full-mining input file
	Part_mining.dat	Partial-mining input file
/100x100	culebra.ibd	IBOUND file
	culebra.ihd	Initial heads
	culebra.top	Culebra top elevations
	culebra.bot	Culebra bottom elevations
	steady.ba6	MF2K basic input file
	steady.bc6	MF2K block-centered input file
	steady.nam	MF2K naming file
	steady.dis	MF2K discretization input file
	steady.oc	MF2K output control file
	steady.lmg	MF2K AMG1R5 solver input file
	dtrkmf.in	DTRKMF file name input
	wippctrl.inp	DTRKMF input file
	/50x50	cNew.ibd
cNew.ihd		Initial heads
cNew.top		Culebra top elevations
cNew.bot		Culebra bottom elevations
steady.ba6		MF2K basic input file
steady.bc6		MF2K block-centered input file
steady.nam		MF2K naming file
steady.dis		MF2K discretization input file
steady.oc		MF2K output control file
steady.lmg		MF2K AMG1R5 solver input file
CMine.mod		Mining-altered T-field from FM.F or PM.F
/R*/[scenario]/ d##r###	dtrk.dbg	DTRKMF debug output file
	dtrk.out	DTRKMF output file
	steady100x100.bud	MF2K budget output
	steady100x100.hed	MF2K head output
	steady100x100.lst	MF2K listing file
	steady50x50_ascii.dat	BA.F ASCII budget output
	steady50x50.bud	MF2K flow budget output
	steady50x50.hed	MF2K head output
	steady50x50.lst	MF2K listing file
	TNew.mod	Mining-altered T-field from REFINE.F

boundary corresponding roughly to the center of Nash Draw is shown in Figure 1 [*not shown*] as a purple line extending from the northern to southern boundaries in the western one-third of the model domain. Model cells falling to the west of this boundary are considered to be inactive in the groundwater flow calculations.

Thus, for the mining field and **DTRKMF** simulations in Task 5, the modeling domain consists of 224 cells in the east-west direction (x-direction), and 307 cells in the north-south direction (y-direction). Each cell is of uniform 100 m size on all sides making the modeling domain 22.4 km wide by 30.7 km tall (Figure 3). The discretization of the flow model domain into 100x100 meter cells leads to a total of 68,768 cells with 14,999 (21.8%) of the cells inactive to the west of the no-flow boundary and 53,769 active cells. This number is nearly a factor of 5 larger than the 10,800 (108x100) cells used in the CCA calculations.

The corner coordinates of the modeling domain in UTM NAD 27 are given in Table (3). The current grid differs from the 1996 grid described in Wallace (1996) in that the previous grid was non-uniform and rotated clockwise approximately 38° from the north-south/east-west alignment. In addition, the previous grid used a non-uniform cell size across the domain with a minimum cell dimension of 100 m square over the LWB area and a maximum cell dimension of 800 m square cells at the corners. The model domains of the 1996 grid and the current grid for both the full- and partial-mining scenarios are shown in Figures (4) and (5), respectively.

For the **DTRKMF** particle tracking simulations, a single particle is tracked from the point $X = 613,597.5$, $Y = 3,581,385.2$ (UTM NAD27) to the LWB for each T-field and replicate/scenario combination (Ramsey et al., 1996, p. 9). The coordinates of the LWB are shown in Table (4).

2.5 Boundary and Initial Conditions

Like the model domain and discretization, the boundary and initial conditions used in Task 5 for the groundwater flow modeling runs using **MF2K** are the same as those used in Task 4, and are described fully in McKenna and Hart (2003b). As a summary, field head data from the year 2000 consisting of 37 head measurements across the modeling domain are interpolated to the computational grid using Kriging. A five-parameter Gaussian function is used to de-trend the head data at which point a Gaussian variogram model

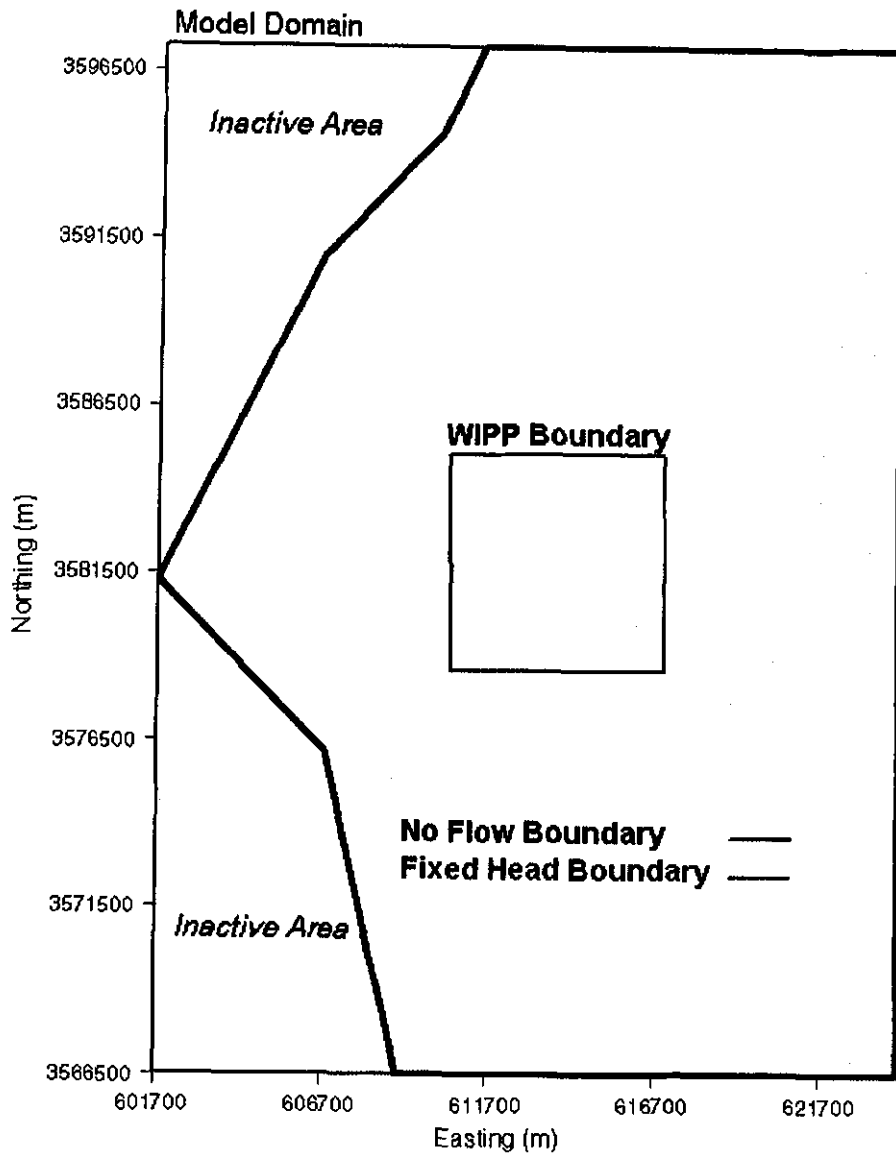


Figure 3: Modeling domain and boundary conditions for the CRA grid configuration. The western no-flow boundary coincides with the groundwater divide underneath Nash draw.

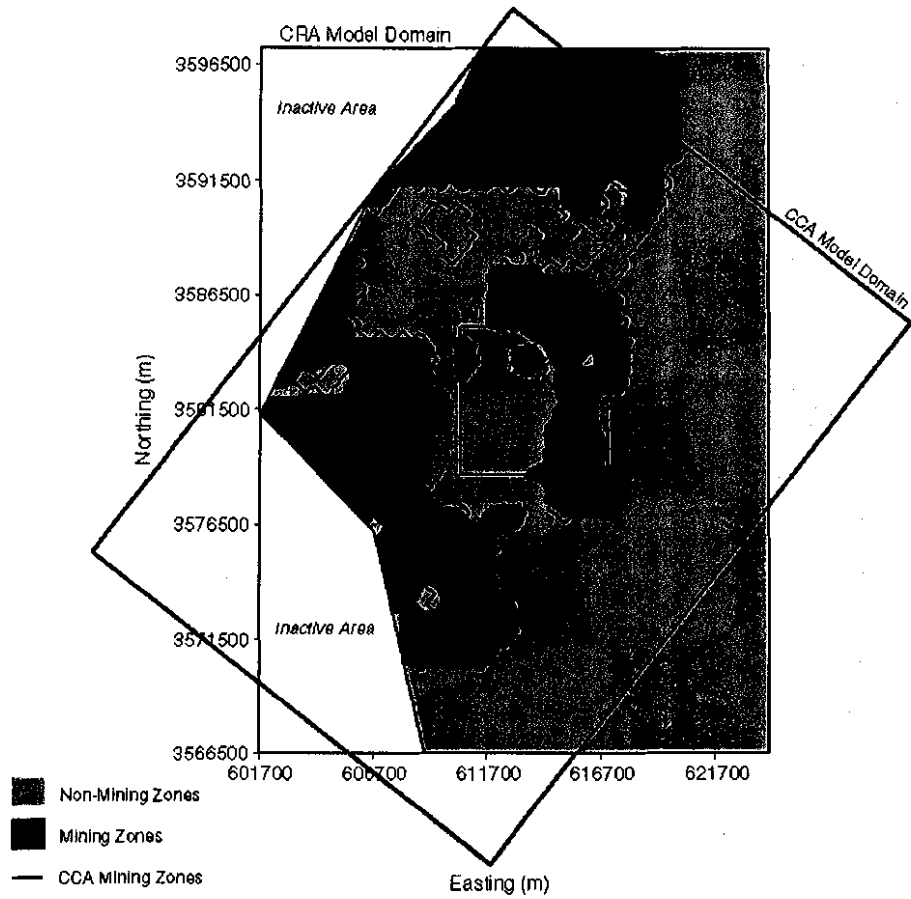


Figure 4: 1996 modeling domain and outline of full-mining zones (red) overlaid on current full-mining zones and modeling domain.

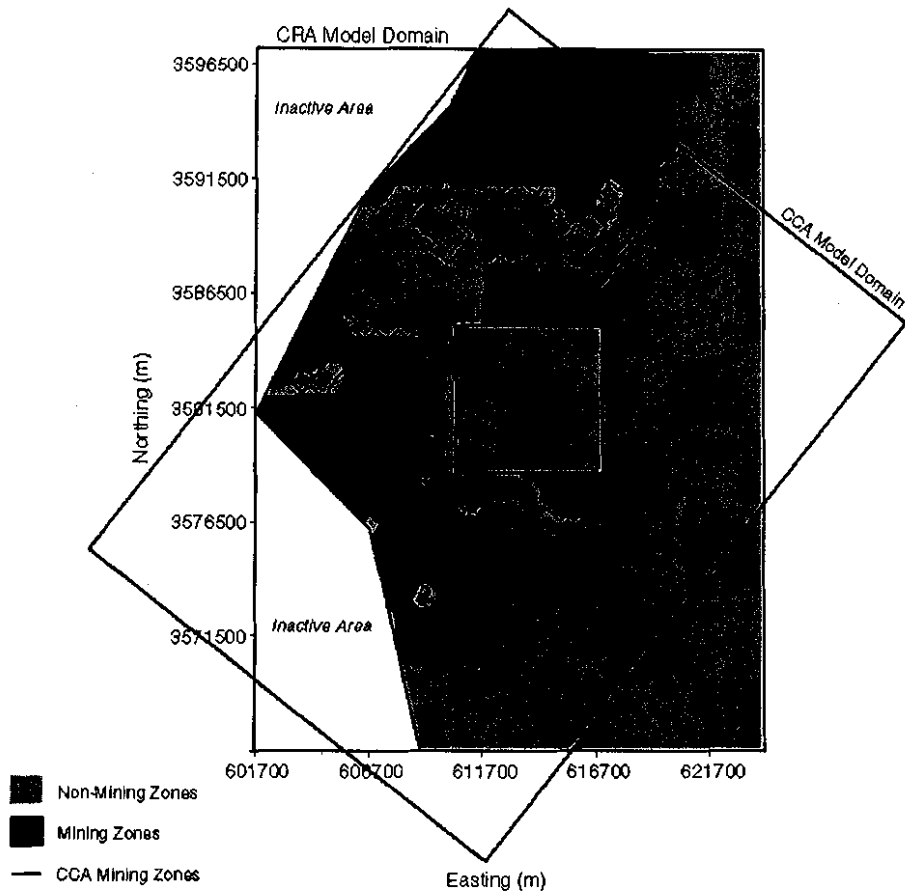


Figure 5: 1996 modeling domain and outline of partial-mining zones (red) overlaid on current partial-mining zones and modeling domain.

Table 3: The coordinates of the corners of the numerical model domain in UTM NAD27 Coordinates.

Domain Corner	X Coordinate (meters)	Y Coordinate (meters)
Northeast	624,100	3,597,200
Northwest	601,700	3,597,200
Southeast	624,100	3,566,500
Southwest	601,700	3,566,500

Table 4: The coordinates of the corners of the WIPP land withdrawal boundary (LWB) in UTM NAD27 Coordinates.

Domain Corner	X Coordinate (meters)	Y Coordinate (meters)
Northeast	616,941	3,585,109
Northwest	610,495	3,585,068
Southeast	617,015	3,578,681
Southwest	610,567	3,578,623

is used to describe the variability of the head residuals with distance. The variogram model is used to estimate the residuals at each node in the grid. The final step is to add the regional trend back to the estimated residuals using the five-parameter Gaussian function.

The model boundaries along the north, east, and south edges of the domain are considered fixed-head boundaries. The Kriged head values to determine the initial heads are assigned to each constant head cell and kept fixed throughout the simulation. Since all simulations for this Task are steady-state, determination of the initial heads are important only in relation to setting the fixed boundary conditions. The irregular western boundary is considered a no-flow boundary and falls roughly along the groundwater divide associated with Nash Draw. Nash Draw is interpreted as a regional groundwater divide, draining the Rustler units to the east and north (and also by implication via discharge symmetry, to the west). The initial head contours across the active modeling domain are shown in Figure (6).

Since the extent of possible potash mining extends well beyond the modeling domain, the effects of mining on the boundary conditions must be considered. Regional flow rates within the flow model are controlled by the

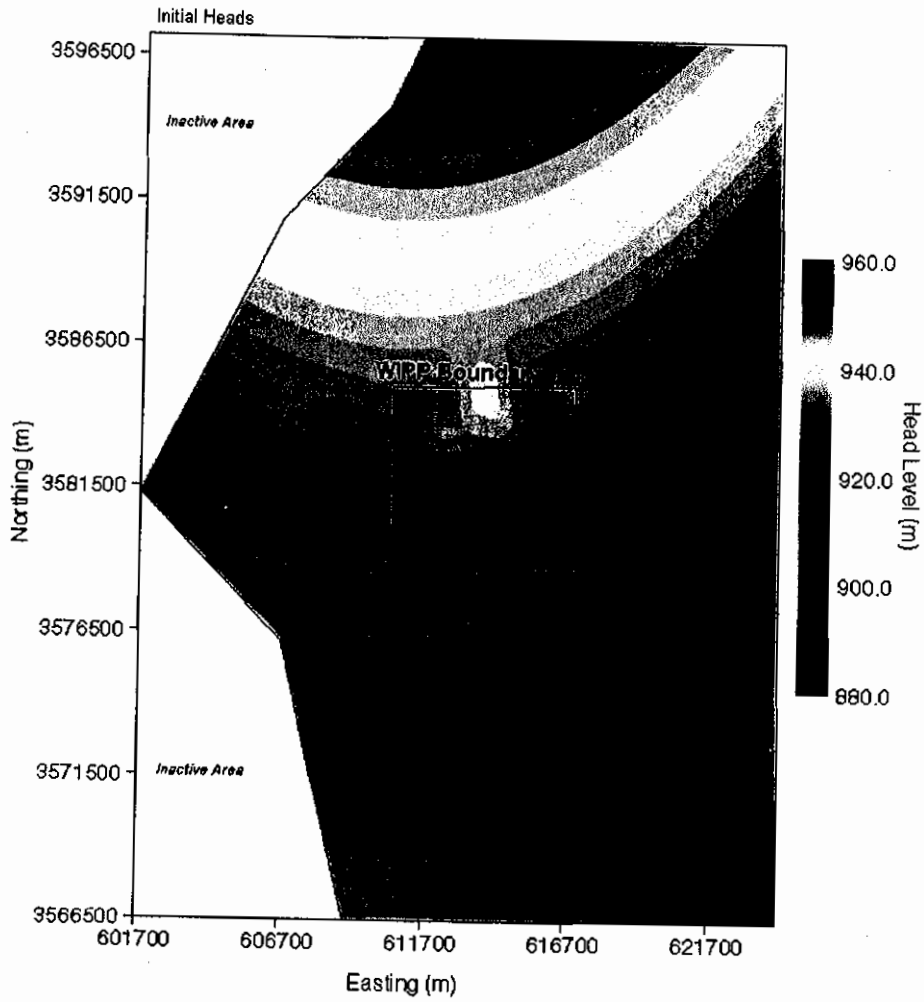


Figure 6: Initial heads across modeling domain.

boundary conditions and the hydraulic conductivity distribution. The regional gradient across the domain is approximately 0.0017, which is higher than the 0.001 quoted in Wallace (1996) for the CCA. It should be noted that the regional gradients are difficult to directly compare since the CCA grid is rotated approximately 38° clockwise from the CRA grid. Thus, for the CCA grid, the regional gradient is calculated by taking the difference of the highest constant head in the northern corner of the model and the lowest constant head in the southern end of the model, and dividing by the distance between these two points. For the current grid we average the constant heads along the northern boundary, subtract the average heads along the southern boundary, and then divide by the north-south model domain distance. Using only the cells with the highest and lowest constant heads and dividing by the distance between the two, as was done with the CCA grid, the regional gradient is calculated to be 0.0022, which overestimates the regional behavior. It is assumed that mining impacts would not significantly change this regional gradient and thus the boundary conditions for the mining scenarios are identical to those in Task 4. In addition, the CCA used the same conceptualization (keeping boundary conditions fixed between the mining and non-mining scenarios) and to allow for comparisons between the CCA and the CRA, the same conceptualization is maintained.

2.6 Subtask 1: Determination of Potential Mining Areas

An updated version of the 1993 BLM map, "Preliminary Map Showing Distribution of Potash Resources, Carlsbad Mining District, Eddy and Lea Counties, New Mexico" (BLM, 1993), was obtained directly from David Hughes of Washington Regulatory Environmental Services (WRES) as an Autocad DXF file (Figure 7). This map was originally developed for the CCA and is periodically updated as part of the "Delaware Basin Drilling Surveillance Program", which is performed by WRES.

The coordinates of the DXF file are in State Plane NAD 27, Region 3001 (New Mexico East), and thus required conversion to the UTM NAD 27 (zone 13) system used in this study. The coordinate conversion was done using the Department of Defense groundwater modeling software, GMS (GMS, 2003). After the coordinate conversion, three coverages were extracted from the DXF file, 'Leases inside the Basin', 'Possible Future Mining', and 'Mining

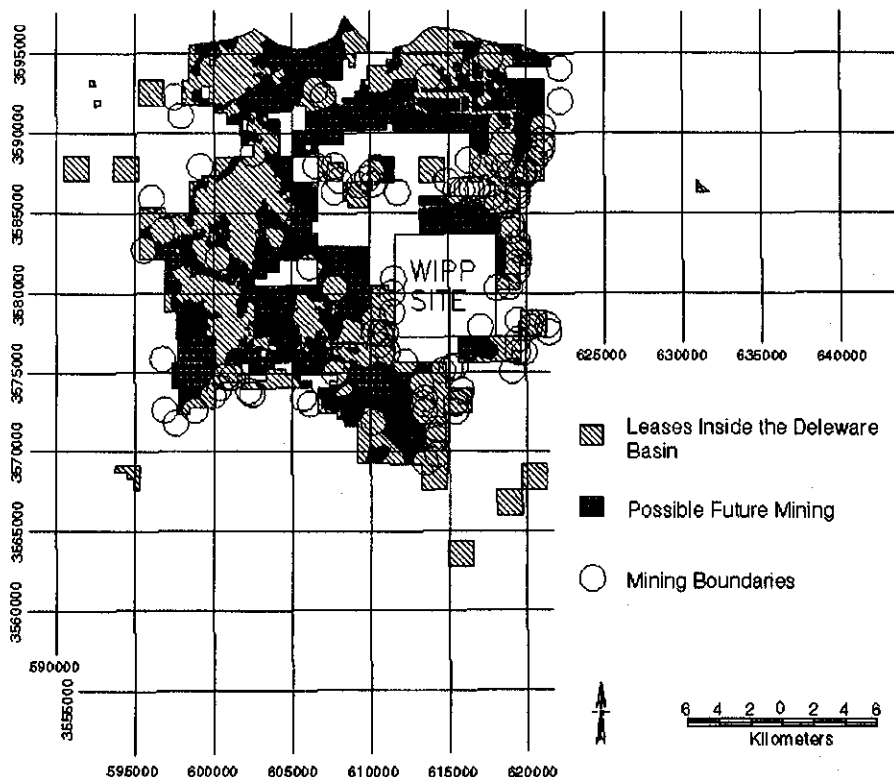


Figure 7: Leased potash resources near the WIPP site. Coordinates are in UTM NAD 27.

boundaries'. The first coverage, 'Leases inside the Delaware Basin', delineates the areas that are leased to mining companies with no determination of whether potash exists in that area or not. However it does contain all areas that have been or are currently being mined. Consequently, this coverage was matched with the second coverage, 'Possible Future Mining' to determine the leased areas that have viable potash resources. The third coverage, 'Mining Boundaries' is a set of one-mile diameter circles around each well drilled for oil and gas exploration. These areas are under control of the oil and gas companies and thus are off limits to potash mining. This means the

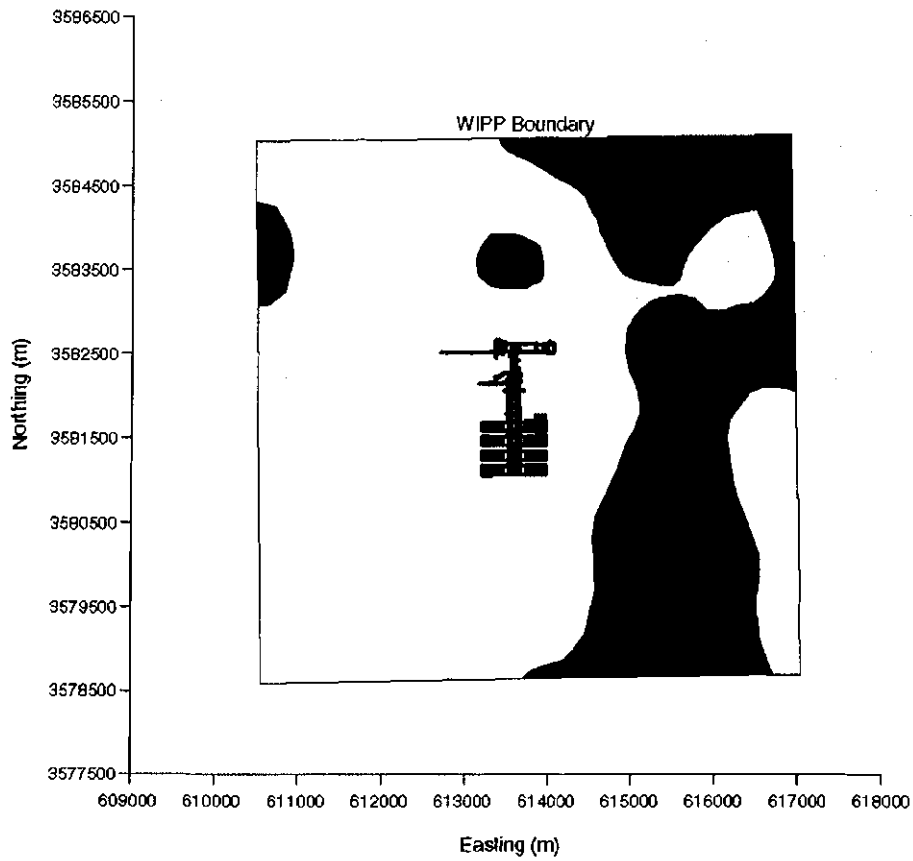


Figure 8: Potential potash distribution within WIPP boundary (red). The repository structure is shown in the center. Coordinates are UTM NAD 27.

YOUNG & RUBICAM

INFORMATION ONLY

third coverage is subtracted from the joining of the first two. The result is a new composite coverage that shows the currently mined and future potential mining areas.

Since the potash mining area is located in the Salado Formation, below the Culebra, the areas disturbed by mining activities in the Culebra are larger than shown on the the BLM map due to subsidence-induced angle-of-draw effects. The rationale for determining the extent of these effects is described in Wallace (1996) with the final conclusion stating that an additional 253 m wide 'collar' was to be added to the mining-impacted areas. This is considered a conservative estimation of the angle-of-draw effects. The new delineation is then compared to the 1996 model mining zones to make sure there are no unexplainable differences. The main differences between the CCA map and the current CRA map created here are from recent oil and gas borehole explorations in the area that have ruled out extraction of potash resources. The current modeling domain and mining zones for the full-mining case are shown in comparison to the 1996 delineation in Figure (4). A closeup of the WIPP site and the associated mining zones is shown in Figure (8). The partial-mining case is shown in Figure (5).

The output of this delineation is a file that contains one value for each cell in the grid. A value of 0 is an inactive cell, a value of 1 means the cell lies within a potential mining zone, and a value of 2 means it lies outside a potential mining zone. One file for each scenario, full-mining and partial-mining, is generated, and used as input to the data conversion programs, **FM.F** and **PM.F** (Appendices A and B) respectively.

2.7 Subtask 2: Use of Mining Zones in Forward Simulations

The calibration process in Task 4 produces a transmissivity field that minimizes the error between the steady-state and transient head distributions and the calculated distributions using the calibrated field. Since the calibration process does not produce a unique solution, i.e. given a different set of starting transmissivities a different final set of transmissivities may be reached, multiple T-fields are produced and 100 are selected based on the criteria set forth in Beauheim (2003). Each selected T-field is multiplied by its own unique mining scaling factor in areas of potential mining, and **MF2K** is run to produce the mining-affected head distribution and the cell-by-cell flow budget files. The cell-by-cell flow budget file is used for input to Subtask 3.

To assure repeatability, three different sets of mining factors are used, each set forming a replicate. Thus, for this Task and for each mining scenario (full and partial), 3 sets of 100 mining-altered T-fields are produced. A list of the qualified runs and the corresponding random mining factor for each replicate is listed in Appendix (J).

2.8 Subtask 3: Particle Tracking using DTRKMF

As explained above in Section 2.4, a single particle is tracked from the point $X = 613,597.5$, $Y = 3,581,385.2$ (UTM NAD27) to the LWB for each T-field and replicate/scenario combination, using the code **DTRKMF**. Two outputs are generated from the suite of particle tracks. First are plots showing the individual tracks for all 100 T-fields in each scenario for each replicate (6 plots total). This allows for visual comparison of the prevailing flow directions for the full- and partial-mining scenarios and the qualitative comparison of the variability of the tracking direction. Secondly, cumulative distribution functions (CDF's) are constructed for each replicate and scenario. The CDF's describe the probability that a particle will cross the LWB in a given amount of time. The six plots and the CDF's are presented below in the results section.

3 Modeling Assumptions

Besides assumptions inherent in all modeling exercises (e.g. physical processes can be adequately parameterized and estimated on a numerical grid) there are several assumptions that are specific and important to this Task. Those assumptions are as follows:

1. It is assumed that the boundary conditions along the model domain boundary are known and are not dependent on mining. The reasoning for this assumption is described in Section 2.5.
2. It is assumed that the flow-field over the duration of the particle tracking and transport times can be adequately represented by steady-state conditions. This is related to the first assumption in that the boundary conditions are also assumed to remain constant over time. This assumption is necessary since data do not exist that can predict the transient conditions at the site over the time frames involved (>100,000 years).
3. It is assumed that the mining effects can be adequately represented with a single mining factor that increases the transmissivity uniformly

across the potential mining zones within the Culebra. This is directed by EPA regulation 40CFR Part 194, p. 5229 and is assumed adequate for this Task. The regulation is included as an appendix in Wallace (1996).

Other assumptions related to this Task can be found in McKenna and Hart (2003b).

4 Results

The effect of mining on transport in the Culebra is difficult to quantify given the high level of uncertainty in the overall conceptualization and the various input parameters. This uncertainty is addressed by the repetitive nature of the simulations: 100 T-fields are passed from Task 1 of AP-100, and 3 replicates across two different mining scenarios are examined for this Task. However, qualitative conclusions are useful in providing insight as to the impacts of mining and thus the results presented here will concentrate more on the qualitative conclusions of this Task rather than specific deductions.

4.1 Particle Travel Times

For both of the mining scenarios, travel times to the LWB are longer than for the non-mining cases; the median travel times across all 3 replicates for the full- and partial-mining scenarios are approximately 3.61 and 2.64 times greater than for the non-mining scenario, respectively. A plot of the cumulative distribution functions (CDFs) for the full-, partial-, and non-mining scenario's is shown in Figure (9).

Given the increase in transmissivity due to mining, the increase in travel time may seem counter-intuitive. However, upon examination of the head contours and flow patterns of the mining cases, the high transmissivity areas corresponding to the mining zones create preferential pathways through the system. Figure (10) shows the normalized velocity in each cell for the T-field/replicate averaged case for the full-mining scenario. The normalized velocity is the velocity magnitude in each cell divided by the maximum velocity magnitude across the domain. Since the velocity magnitudes are highly skewed, the color bands for Figure (10) are non-uniformly scaled at the high end (i.e. a wider range of velocity magnitudes is used to designate the orange and red bands). This allows for a better qualitative comparison of the

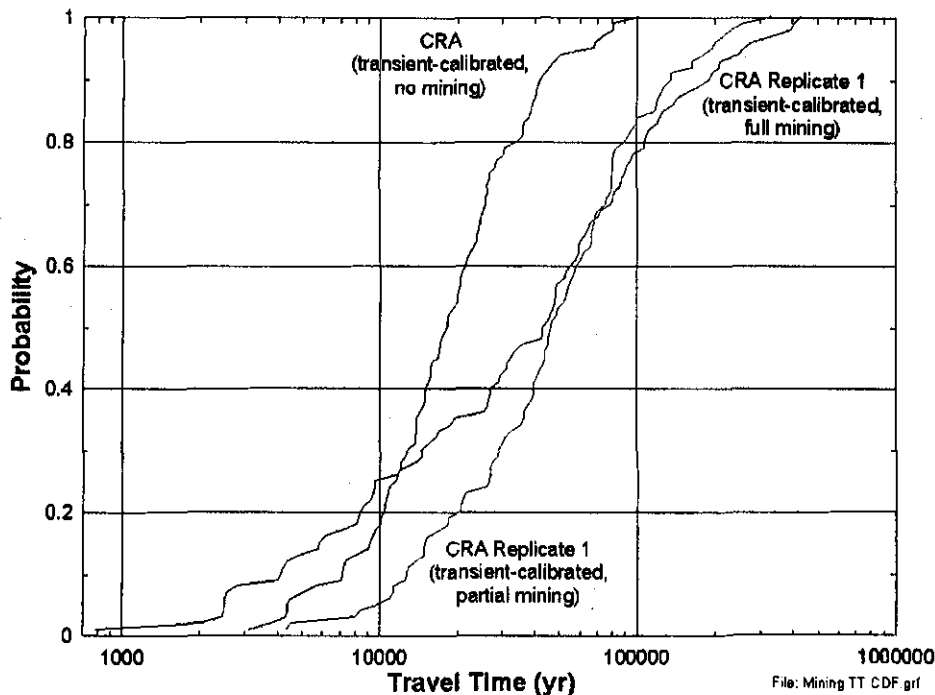


Figure 9: Cumulative distribution function plot of the full-, partial-, and non-mining scenarios for the CRA.

spatial distribution of high and low velocities. 'T-field/replicate averaged' means the transmissivity value for each cell is the average of the transmissivities across all T-field/replicate combinations for the full-mining scenario (300 T-fields in total). Not surprisingly, it is clear that the areas of high velocities correspond with the mining zones. The higher velocities and corresponding higher flow rates through the mining zone areas translate to slower velocities in the non-mining zone areas. In most cases, the particles for the mining-scenarios stay in the lower velocity zones along the entire pathway to the LWB, which accounts for the higher average travel times. A comparison of the median, maximum, and minimum values for the full-, partial-, and non-mining scenario travel times is presented in Table (5).

A comparison to the compliance certification application (CCA) results is useful to provide perspective on the impact of the changes between the CCA

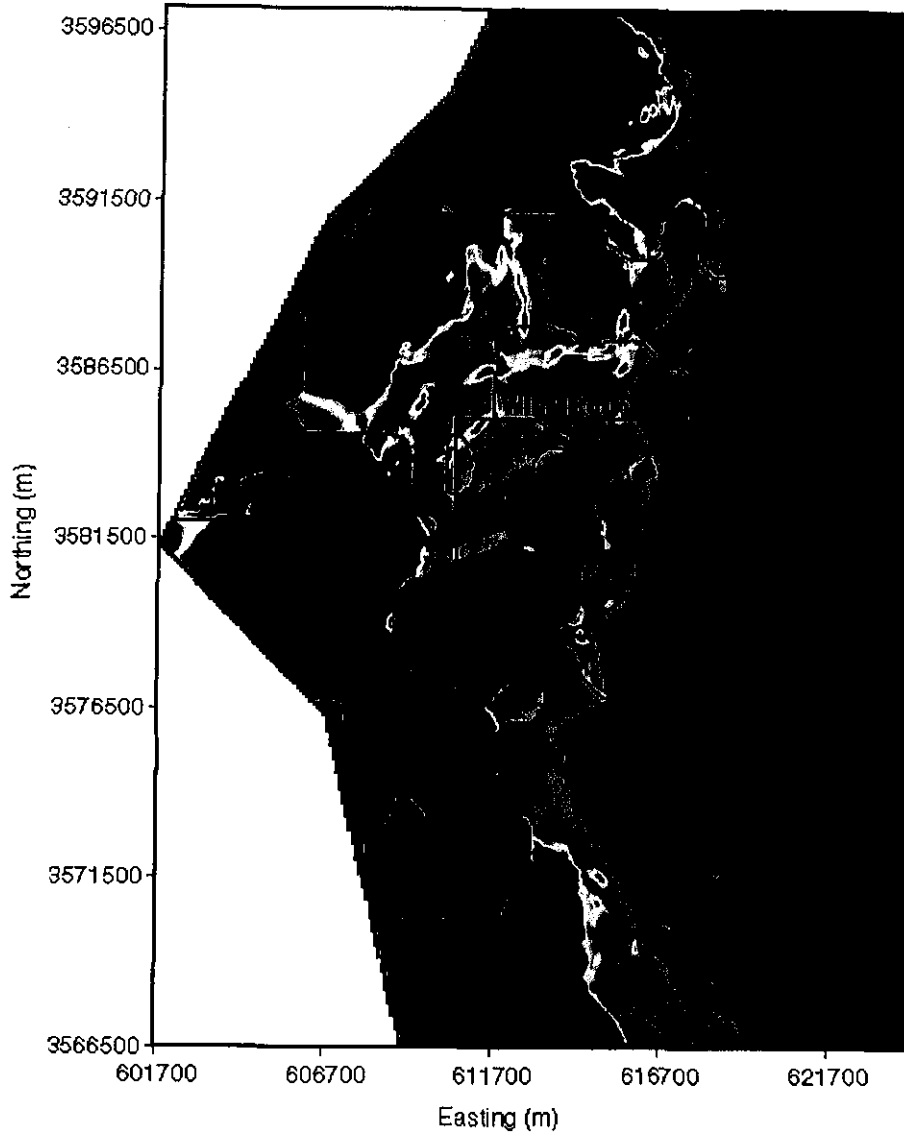


Figure 10: Normalized pore velocities for the full-mining case. Red indicates zones of high velocity. The black lines show the full-mining zones and the red box is the WIPP LWB. The T-field used to produce the velocity profile is averaged across all T-field/replicate combinations for the full-mining scenario (300 T-fields in total).

Table 5: Travel time statistics in years for the full and partial mining scenarios as compared to the non-mining scenario from Task 4.

Replicate	Stat	Full	Partial	Non
R1	Med.	63,370	47,745	NA
	Max.	504,174	494,981	
	Min.	723	4,684	
R2	Med.	73,169	47,651	
	Max.	3,387,185	531,136	
	Min.	611	4,654	
R3	Med.	63,430	51,622	
	Max.	1,610,979	506,437	
	Min.	615	4,603	
Global	Med.	66,048	48,290	18,289
	Max.	3,387,185	531,136	101,205
	Min.	611	4,603	3,111

and the CRA. Figures (11) and (12) show the full- and partial-mining scenarios, respectively, for all three replicates as compared to the CCA results. The CRA travel times are approximately 2.2 and 3.5 times longer for the full- and partial-mining scenarios, respectively, than for the CCA scenarios. This is mainly due to the difference in how the base T-fields are generated. The CCA fields use a categorical simulation technique to capture both high transmissivity (T) and low T regions. In contrast, the CRA fields incorporate more geological understanding, with regions to the west categorized as high T, regions to the east categorized as low T, and the area in between given high or low T on a stochastic basis. This results in significant differences in T in the southern part of the WIPP site. The CCA fields tend towards lower and more uniformly distributed T's in the southwestern portion of the WIPP site, and a high T channel down the southeastern part of the site that leads to shorter travel times than the CRA. The CRA fields show higher T's in the southwestern part of the WIPP site and tend not to have the high T channel in the southeast, causing travel times to increase.

Another interesting point illustrated by Figures (11) and (12) is the similarity between the 3 replicates for the CRA curves. This indicates that the use of 100 T-fields from Task 1 of AP-100 is adequate to capture the mean

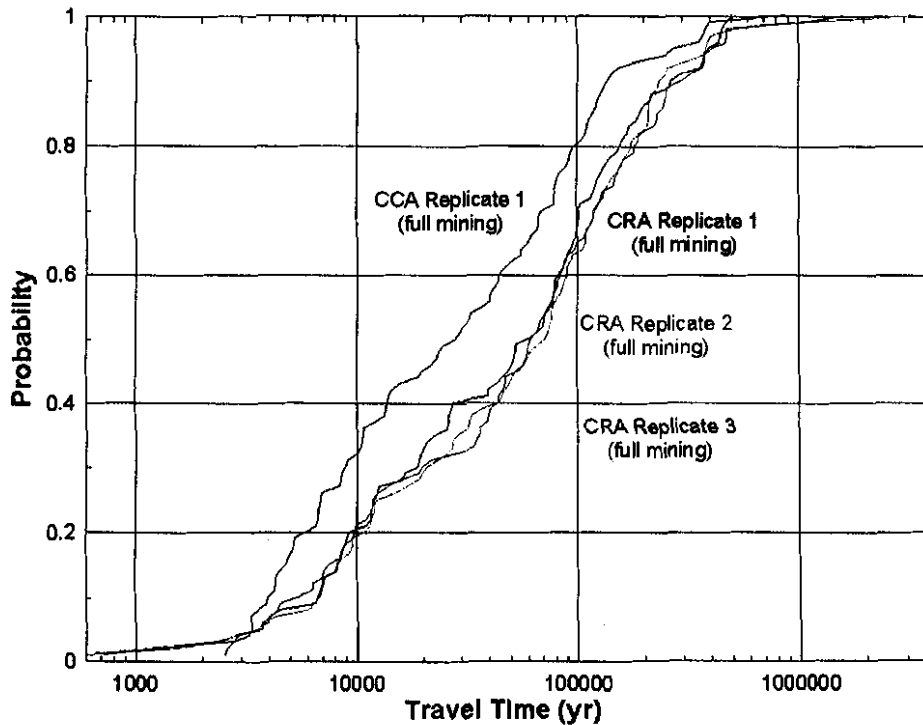


Figure 11: Cumulative distribution function plot of the 3 full-mining scenario replicates as compared to the CCA full-mining scenario. An increase in travel time can be seen for the CRA scenarios.

behavior of the mining effects.

4.2 Travel Direction

The effects of mining also have an impact on the direction of transport, significantly changing where the particles cross the LWB. This is especially true of the full-mining scenario where mining within the LWB creates high head along the eastern boundary of the WIPP resulting in a general flow direction to the west-southwest. This is in contrast to the partial-mining scenario where the tracking direction is mainly towards the south, similar to the non-mining scenario. The particle track directions for the full- and

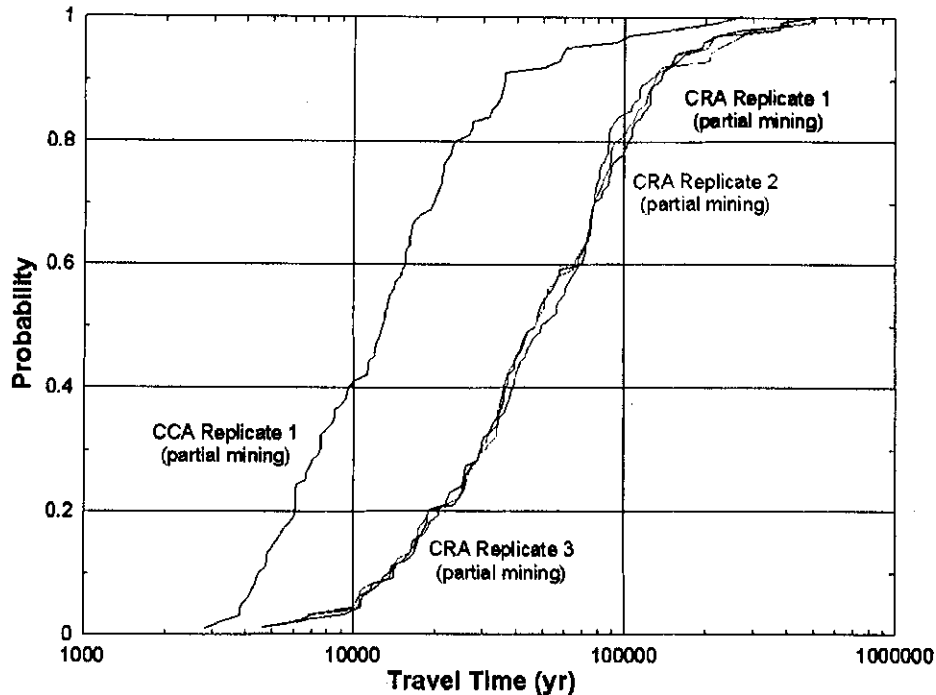


Figure 12: Cumulative distribution function plot of the 3 partial-mining scenario replicates as compared to the CCA partial-mining scenario. An increase in travel time can be seen for the CRA scenarios.

partial-mining scenarios are illustrated in Figures (13) to (18). There is a strong similarity within each replicate for each scenario. Individual tracks can be recognized from one replicate to the next, with some slight variations. This indicates that track directions are determined more by the spatial variation of the calibrated T-field than by the random mining factors. As long as there is *some* (see below) increase in the mining zone transmissivities over that of the non-mining areas, the tracks for each T-field will be similar from one replicate to the next.

The insensitivity of the track directions to the random mining factor also carries over to insensitivity of the travel time. Correlation analysis shows correlations between travel time and the random mining factor for the full and partial-mining scenarios as 0.091 and 0.151, respectively. Thus, like the

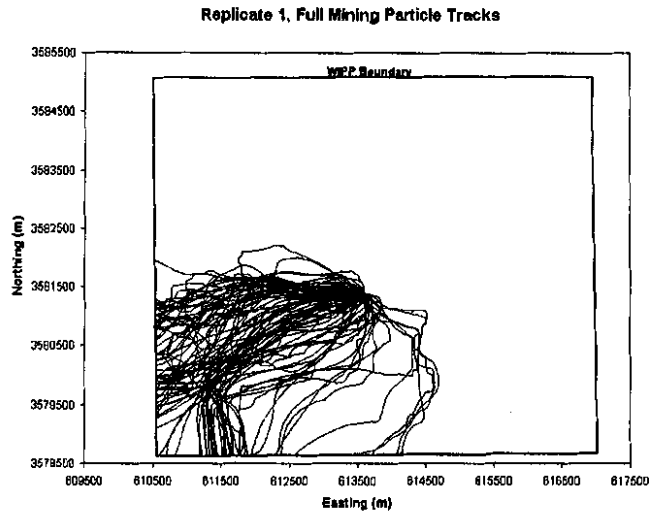


Figure 13: Particle tracks for replicate 1 for the full-mining scenario.

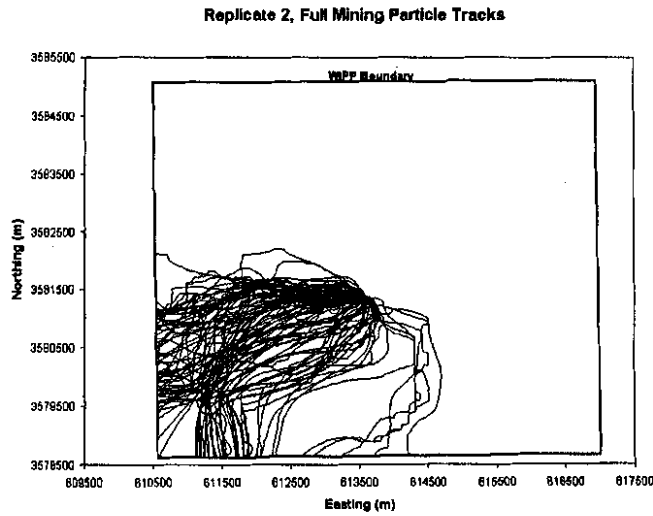


Figure 14: Particle tracks for replicate 2 for the full-mining scenario.

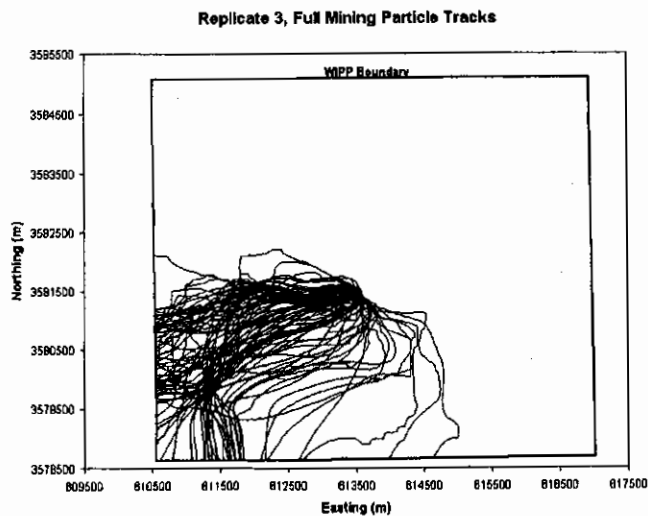


Figure 15: Particle tracks for replicate 3 for the full-mining scenario.

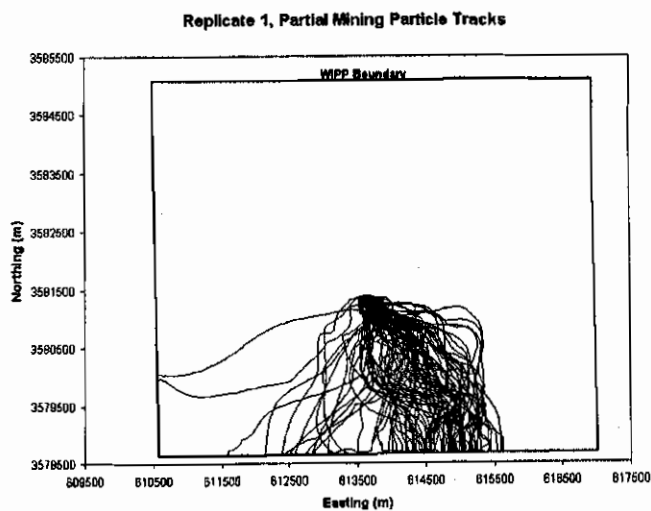


Figure 16: Particle tracks for replicate 1 for the partial-mining scenario.

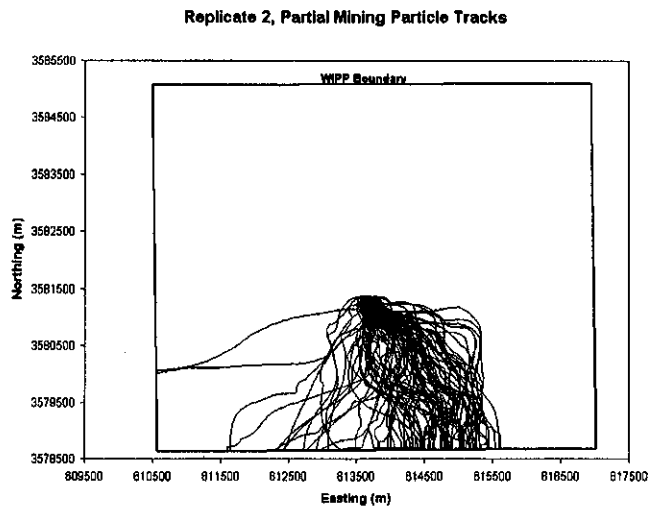


Figure 17: Particle tracks for replicate 2 for the partial-mining scenario.

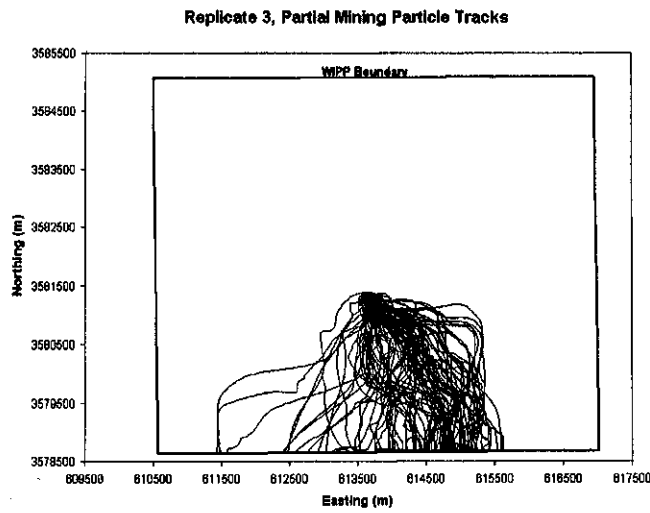


Figure 18: Particle tracks for replicate 3 for the partial-mining scenario.

track directions, travel times are not sensitive to the random mining factor but rather to the spatial structure of the calibrated T-field.

This insensitivity to the random mining factor can be explained by recalling that the factor is applied only to zones deemed as probable mining areas. This means that velocity and flow increases are limited to the mining zones, with little change in the non-mining areas (assuming gradients are somewhat constant). Conditions within the non-mining zones are affected most for cases where the mining zone transmissivities are close to the non-mining zone transmissivities. However, the mining factor ranges uniformly from 1-1000 meaning 99% of the T-field/replicate combinations will have multipliers greater than one order of magnitude (for the 300 combinations in this Task, only two have multipliers that are less than 10). This translates into small changes within the non-mining zones for relatively large changes in the mining zones. To illustrate this, Figure (19) shows the Log_{10} travel times versus the random mining factor for the full- and partial-mining scenarios across all replicates. The high scatter in both the plots is due to the independence of travel time with regards to the mining factor. This conclusion supports the mining scenario conceptual model and the use of a random mining factor to model changes in transmissivity due to mining activities. It also indicates that the controlling parameters are the spatial distribution of the non-mining scenario T-field and the delineation of the mining and non-mining zones.

4.3 Extreme Values

Examination of the extreme travel time values, and the causes behind those values, is useful in quantifying the range of outcomes given the amount of uncertainty incorporated into the models. For the full-mining scenario, T-field d04r01 from replicate 2 had the longest travel time of 3,387,185 years. In contrast, T-field d01r07 from replicate 2 had the shortest travel time of 611 years. The median travel time (66,215 years) is best represented by T-field d10r09 in replicate 1. Figures 20 to 22 show the head contours for each of these cases along with the corresponding particle track. What distinguishes the plots is the head distribution across the regions. For the slow case (Figure (20)) the head contours to the west of the repository are spread far apart, indicating a low gradient and thus lower groundwater velocities. The fastest case (Figure (21)) shows a high-gradient band that originates along the no-flow boundary to the northwest and runs down the western side of the WIPP site. This high gradient corresponds to higher groundwater velocities. The

THIS INFORMATION IS UNCLASSIFIED

INFORMATION ONLY

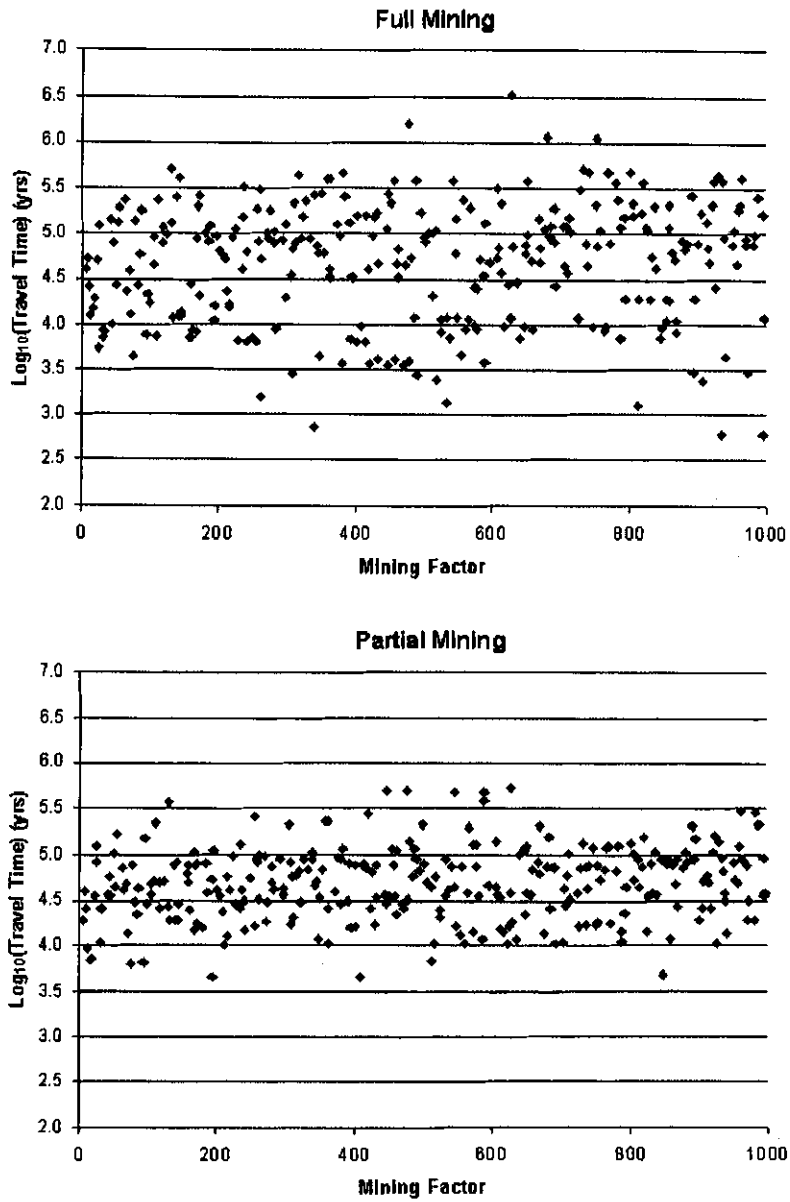


Figure 19: Correlation between the random mining factor and Log-travel time.

median case (Figure (22)) also shows this high-gradient band but it is not as extreme as in the fast case. In all cases, the mining-zone areas look very similar, with widely spaced head contours and higher velocities relative to the non-mining zones.

The partial-mining cases have similar characteristics to that of the full-mining cases (Figures 23 to 25) except that the band of high gradient to the northwest is more pronounced and persistent. The slowest partial-mining T-field is d04r01 (Figure (23)) from replicate 2 (531,136 years), the fastest is d08r01 (Figure (24)) from replicate 3 (4,603 years), and the median is best represented by d01r04 (Figure (25)) from replicate 1 (48,472 years). The particle tracking directions are more similar between each other in the partial-mining case than in the full-mining cases. Overall, for both the full and partial-mining scenarios, those T-fields that contain higher and more heterogeneous transmissivities in the non-mining areas produce the fastest travel times. However, the partial-mining scenario shows a smaller range of values due to the lack of the large mining zone in the WIPP area. This smaller range is clearly visible in Figure (19).

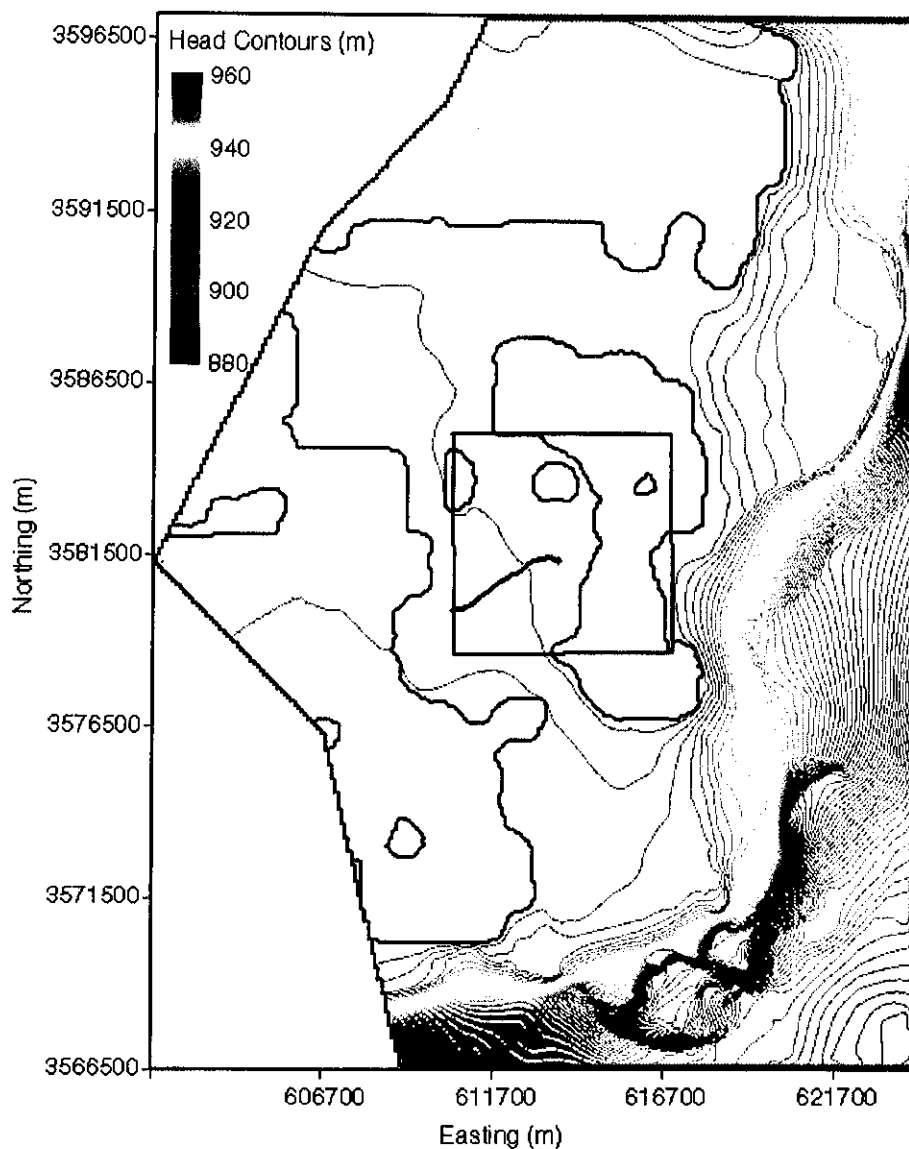


Figure 20: Head contours and particle track for the maximum travel time T-field (d04r01-R2) for the full-mining case. The WIPP boundary is the red box in the center of the figure and the particle track is the blue track originating from the approximate center of the WIPP.

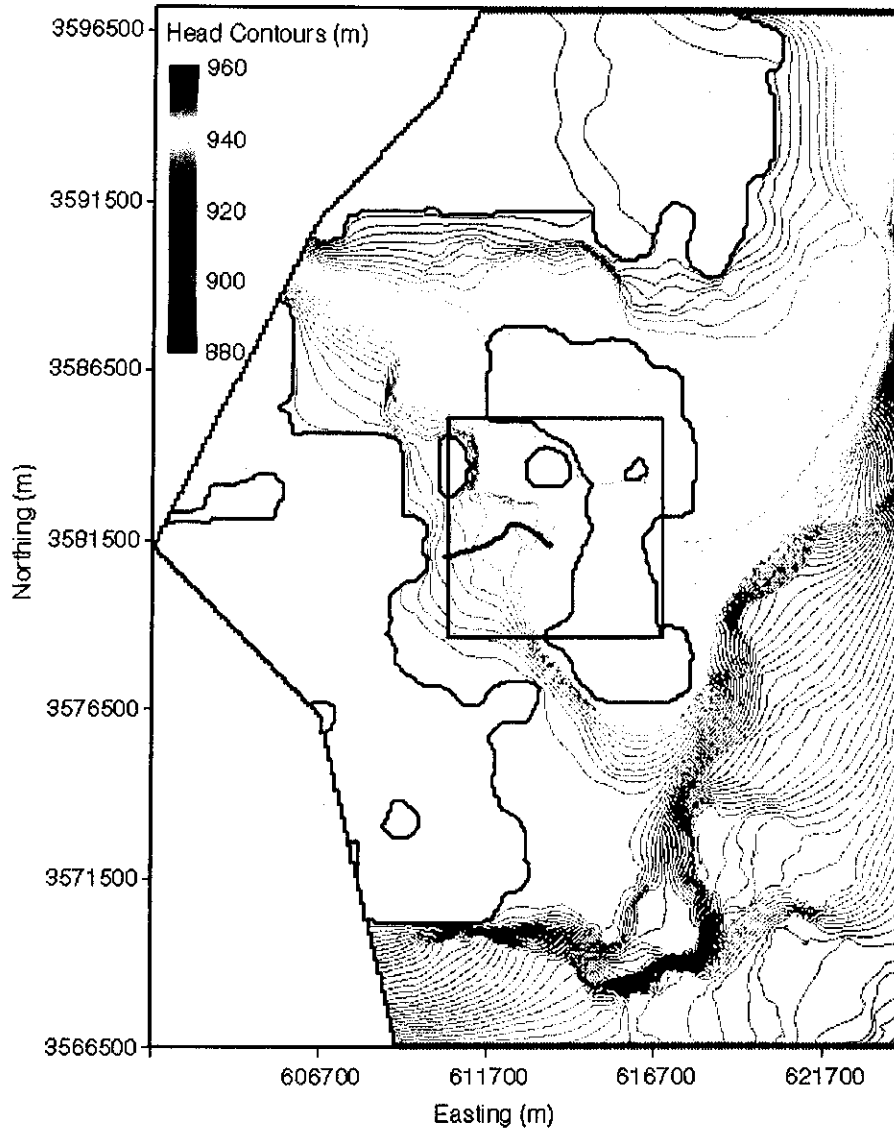


Figure 21: Head contours and particle track for the minimum travel time T-field (d01r07-R2) for the full-mining case. The WIPP boundary is the red box in the center of the figure and the particle track is the blue track originating from the approximate center of the WIPP.

UNCLASSIFIED

INFORMATION ONLY

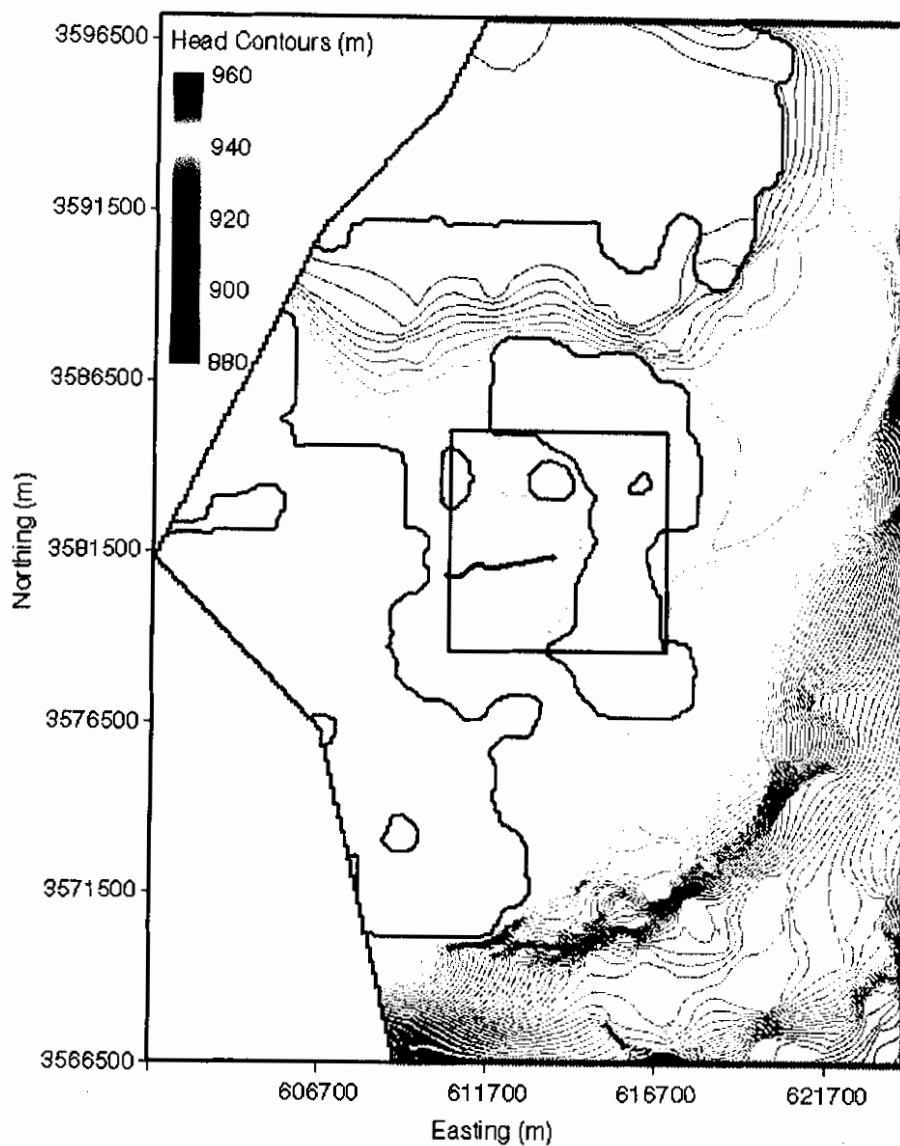


Figure 22: Head contours and particle track for the median travel time T-field (d10r09-R1) for the full-mining case. The WIPP boundary is the red box in the center of the figure and the particle track is the blue track originating from the approximate center of the WIPP.

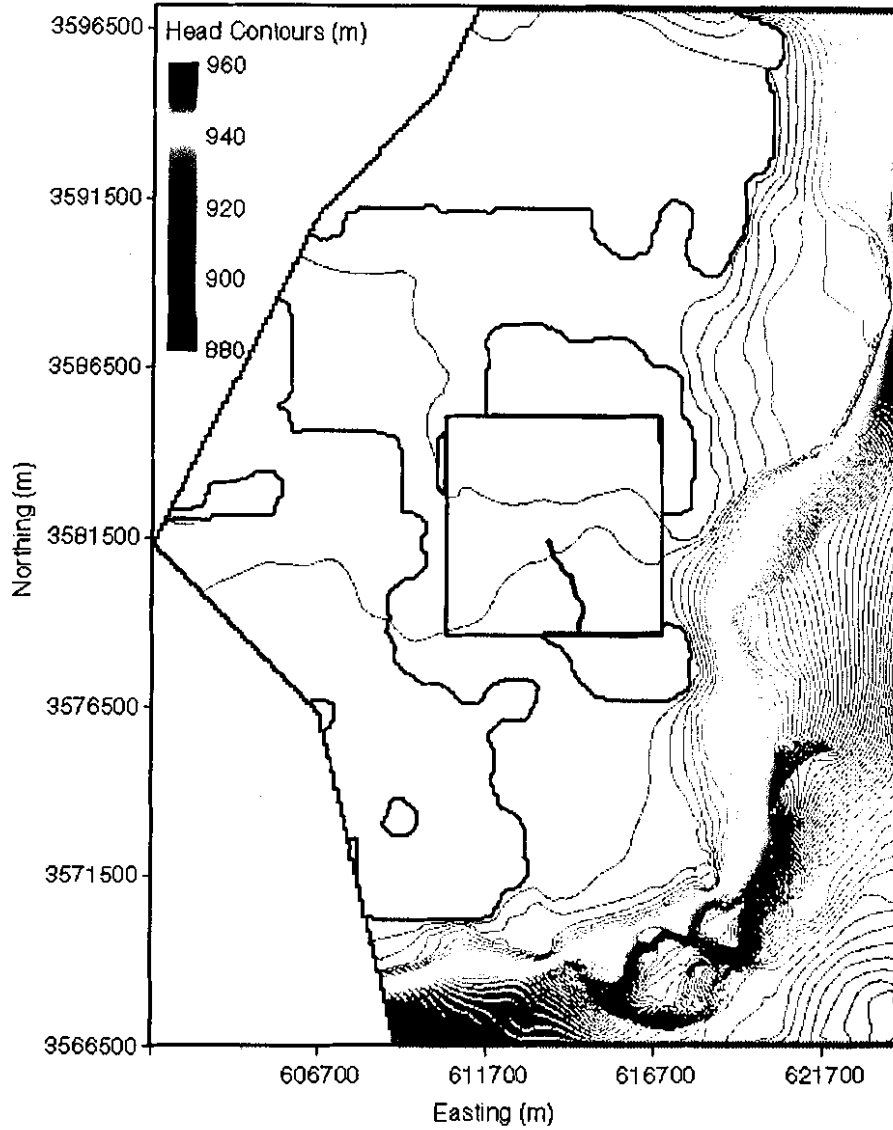


Figure 23: Head contours and particle track for the maximum travel time T-field (d04r01-R2) for the partial-mining case. The WIPP boundary is the red box in the center of the figure and the particle track is the blue track originating from the approximate center of the WIPP.

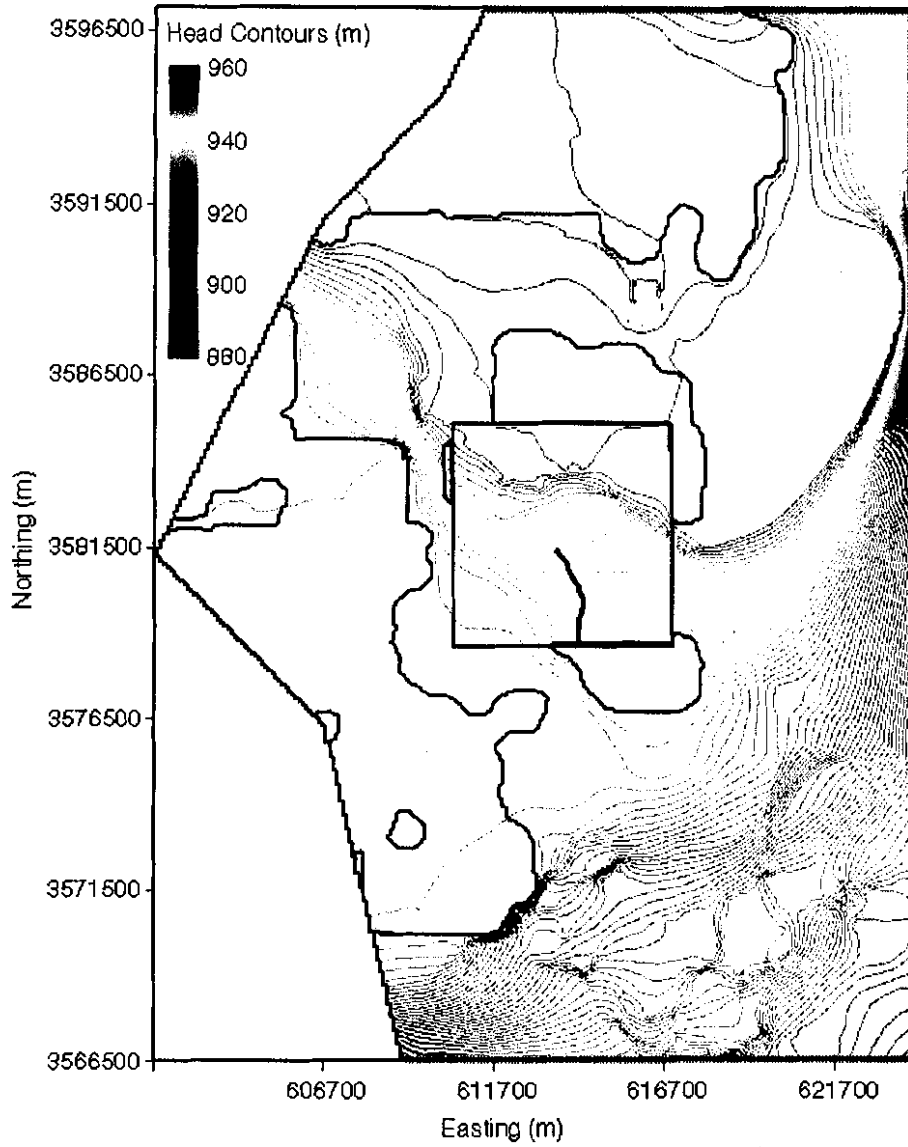


Figure 24: Head contours and particle track for the minimum travel time T-field (d08r01-R3) for the partial-mining case. The WIPP boundary is the red box in the center of the figure and the particle track is the blue track originating from the approximate center of the WIPP.

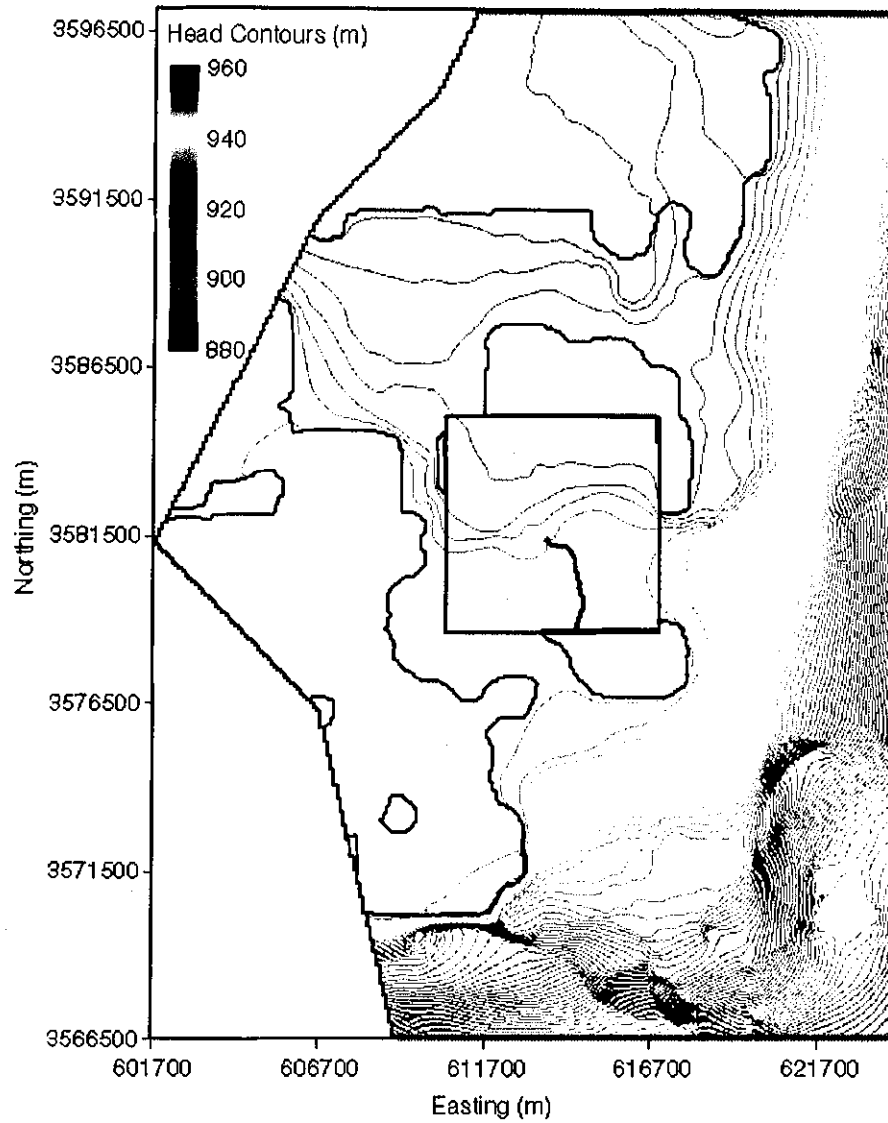


Figure 25: Head contours and particle track for the median travel time T-field (d01r04-R1) for the partial-mining case. The WIPP boundary is the red box in the center of the figure and the particle track is the blue track originating from the approximate center of the WIPP.

5 Summary

This Task (Task 5) of AP-088, Analysis Plan for Evaluation of the Effects of Head Changes on Calibration of Culebra Transmissivity Fields, investigates the impact of the increase in transmissivity in the Culebra due to potash mining in and around the WIPP regional area. To accomplish this investigation, two categories of mining-impacted transmissivity fields are modeled: one with mining outside the land withdrawal boundary (LWB) only and the other with regions both inside and outside the LWB mined (partial and full-mining scenario's, respectively).

The impacts are modeled by scaling each calibrated T-field passed from Task 1 of AP-100 in regions deemed to contain economically-extractable potash resources by a random factor between 1 and 1000. A forward steady-state flow model is run for each new T-field under each mining scenario (full and partial) across three replicates, resulting in 600 simulations (there are 100 calibrated T-fields from Task 1 of AP-100). Particle tracking is performed on the modified flow fields to determine the flow path and groundwater travel time from a point above the center of the WIPP disposal panels to the LWB. Cumulative probability distribution functions (CDF) are produced for each mining scenario and compared to the undisturbed scenario generated from Task 4 of AP-088, as well as to the full- and partial-mining scenarios from the 1996 CCA. The CDF's describe the probability of a conservative tracer reaching the LWB at a given time. In addition to comparing travel times, particle tracking directions are also examined to determine the effect on the regional flow direction in the WIPP area due to mining. The flow fields generated from the mining scenarios are then refined and passed to Task 6 of AP-100 that performs radionuclide transport modeling in the Culebra.

Results show that for both the full- and partial-mining scenarios, the median particle travel times of 66,215 and 48,472 years are 3.61 and 2.64 times longer than for the non-disturbed case (18,289 years). The increase in transmissivity due to mining in the potential mining zones increases the relative flow rate through these zones, with a corresponding decrease in flow through the non-mining zones. This decrease in flow through the non-mining zones accounts for the longer travel times in the two mining scenarios. Comparing the full- and partial-mining scenarios from the CRA to the CCA, the median travel times are approximately 2.2 and 3.5 times longer, respectively, for the CRA scenarios. This is due to the difference in how the base T-fields are generated between the CCA and the CRA. The CCA fields use a categori-

cal simulation technique to capture both high transmissivity (T) and low T regions while the CRA fields incorporate more geological understanding and stochastic factoring of uncertainty. The net result is longer travel times to the LWB.

No correlation was found between the travel time or the flow direction to the random mining factor. This indicates that even small increases ($\approx 2 - 5$ times) in transmissivity in the mining zone areas are enough to shift the regional flow from a non-mining gradient to a mining gradient. As the mining factor is increased beyond that point (298 out of 300 mining factors are greater than 10) the flow rate and velocities in the mining zones also increase, but with little impact on the non-mining zones or the regional flow directions.

NO NOTATION

INFORMATION ONLY

References

- Beauheim, R. L., 2002. Analysis Plan for Evaluation of the Effects of Head Changes on Calibration of Culebra Transmissivity Fields. AP-088, Rev. 1, 12/06/02, 11 pp., ERMS #524785.
- Beauheim, R. L., 2003. Analysis Report for AP-100 Task 1: Development and Application of Acceptance Criteria for Culebra Transmissivity (T) Fields. Carlsbad, NM: SNL, ERMS # 531136.
- BLM, 1993. Preliminary Map Showing Distribution of Potash Resources, Carlsbad Mining District, Eddy and Lea Counties, New Mexico. Roswell District, U.S. Bureau of Land Management (BLM).
- GMS, 2003. Groundwater Modeling System: Developed by the Environmental Modeling Research Laboratory of Brigham Young University in partnership with the U.S. Army Engineer Waterways Experiment Station, Vicksburg, MS 39180. <http://chl.wes.army.mil/software/gms/default.htm>.
- Harbaugh, A. W., Banta, E., Hill, M. C., McDonald, M., 2000. MODFLOW 2000: The U.S. Geological Survey Modular Ground-Water Model - User Guide to Modularization Concepts and the Ground-Water Flow Process. U.S. Geological Survey, Reston, VA, open file report 00-92, 121pp.
- Helton, J. C., Bean, J. E., Berglund, J. W., Davis, F. J., Economy, K., Garner, J. W., Johnson, J. D., MacKinnon, R. J., Miller, J., O'Brien, D. G., Ramsey, J. L., Schreiber, J. D., Shinta, A., Smith, L. N., Stoetzel, D. M., Stockman, C., Vaughn, P., 1998. Uncertainty and sensitivity analysis results obtained in the 1996 performance assessment for the waste isolation pilot plant. Sandia National Laboratories, SAND98-0365.
- Helton, J. C., Marietta, M., 2000. The 1996 performance assessment for the waste isolation pilot plant, special issue of: *Reliability Engineering and System Safety*. July-September 2000, 69 (1-3).
- Holt, R. M., Yarbrough, L., 2003. Addendum 2 to Analysis Report, Task 2 of AP-088, Estimating Base Transmissivity Fields. ERMS #529416.
- Leigh, C., Beauheim, R. L., Kanney, J. F., 2003. Analysis Plan for Calculations of Culebra Flow and Transport: Compliance Recertification Appli-

- cation, AP-100, Revision 0. Carlsbad, NM: Sandia National Laboratories. ERMS # 530172.
- Lowry, T. S., 2003. Analysis Report of Tasks 2 and 3 of AP-100, Grid Size Conversion and Generation of SECOTP2D Input; Analysis Package for Calculations of Culebra Flow and Transport: Compliance Recertification Application. Carlsbad, NM: Sandia National Laboratories. ERMS # 531137.
- McKenna, S. A., Hart, D., 2003a. Analysis Report, Task 3 of AP-088, Conditioning of Base T Fields to Steady-State Heads. Sandia National Laboratory. ERMS #529633.
- McKenna, S. A., Hart, D., 2003b. Analysis Report, Task 4 of AP-088, Conditioning of Base T Fields to Transient Heads. ERMS #531124.
- Ramsey, J., Wallace, M. G., Jow, H.-N., 1996. Analysis Package for the Culebra Flow and Transport Calculations (Task 3) of the Performance Assessment Analysis Supporting the Compliance Certification Application. Analysis Plan 019, Version 00, ERMS #240516.
- Rudeen, D. K., 2003. Users Manual for DTRKMF, Version 1.00. ERMS #523246. Carlsbad NM: Sandia National Laboratories, WIPP Records Center.
- Wallace, M. G., 1996. Record of FEP screening work, FEP ID# NS-11: Subsidence associated with mining inside or outside the controlled area. ERMS #240816.
- WIPP_PA, 2003a. Analysis Report for the 8400 Regression Test. Sandia National Laboratories, ERMS # 525278.
- WIPP_PA, 2003b. Analysis Report for the ES40 Regression Test. Sandia National Laboratories, ERMS # 525278.
- WIPP_PA, 2003c. Analysis Report for the ES45 Regression Test. Sandia National Laboratories, ERMS # 525278.
- WIPP_PA, 2003d. WIPP PA Design Document for DTRKMF, Version 1.00. Sandia National Laboratories, ERMS #523244.

Appendix A: Full Mining Conversion Code, FM.F

```
!Conversion program for full mining case. This program reads two data sets,  
!Tupdate.mod and full_mining.dat. Tupdate.mod contains the calibrated t-fields  
!from Task 4. Full_mining.dat is a digitized file consisting of a single integer  
!for each cell in the grid: 0 - inactive, 1 - mining zone, 2 - nonmining zone.  
!The transmissivities in the mining areas are then multiplied by a random number  
!between 1 and 1000 to simulate the random increase in transmissivity caused by  
!mining disturbance. The new t-field values are output to an ascii file for input  
!to MODFLOW. Two other parameter files are read, Good_runs.txt and mfr*.txt.  
!Good_runs.txt contains the list of calibrated T-fields from Task 4 and  
!mfr*.txt contains the random mining factors for each replicate. R* is either  
!R1, R2, or R3, depending on the replicate number.  
!Variable list:  
!dx,dy = cell dimension in the x and y directions  
!nx,ny = number of cells in the x and y directions  
!imine = input array of mining, non-mining, and inactive zones  
!trans = input array of calibrated t-field from Task 4  
!rnum = input variable of random mining multiplier  
!file1 = name of mining zone input file  
!file1a = name of replicate file  
!file2 = name of finished run file  
!file2a = name of finished run  
!file3 = name of random mining factor input file  
!file5 = name of t-field input file  
!file6 = name of modified t-field output file  
!path1 = name of local directory  
!path2 = name of remote t-field directory  
!path1f2a6 = path1 + "full" + file2a + file6  
!path22a5 = path2 + file2a + file5  
!5/7/03 - Thomas S Lowry !Modified 6/27/03, 8/12/03 - TSL
```

```
PROGRAM FM_Main  
PARAMETER(dx=100,dy=100,nx=224,ny=307)  
INTEGER imine(nx,ny)  
REAL*8 trans(nx,ny),rnum(100)  
REAL no_min_hd(nx,ny),min_hd(nx,ny)  
  
CHARACTER*40 file1,file2,file2a,file3,file5,file6  
CHARACTER*12 fname,filz  
CHARACTER*55 path1,path2,path1f2a6,path22a5  
CHARACTER*2 rep  
  
!Input file names  
DATA file1/"Full_mining.dat"/  
DATA file2/"Good_runs.txt"/  
DATA file5/"Tupdate.mod"/  
DATA file6/"CMine.mod"/  
DATA path2/"h/wipp/data"/  
  
!Get replicate number  
READ(*,*)rep  
file3="mf"//rep//".txt"  
  
!Set base path  
path1="/home3/tslowry/wipp/mining"//rep//"
```

```
!Open mining file and read mining zones
OPEN(11,file=TRIM(file1),status='old')
DO j=1,ny
  READ(11,*)(imine(i,j),i=1,nx)
END DO
CLOSE(11)

!Open file of finished t-field calibration runs
OPEN(12,file=TRIM(ADJUSTL(file2)),status='old')

!Read random mining factor
OPEN(13,file=TRIM(ADJUSTL(file3)),status='old')
READ(13,*)istop
DO i=1,istop
  READ(13,*)idumb,rnum(i)
END DO

!Read each finished t-field run, if end of file, go to end
DO ifinished=1,1000
  READ(12,'(a6)',END=5000)file2a

!Open calibrated t-field file and read in transmissivities
!Note: cell counting is based on MODFLOW grid, i.e. x-direction
!is left to right and y-direction is top to bottom.
  path22a5=TRIM(ADJUSTL(path2))/TRIM(ADJUSTL(file2a))//"/"//
  & TRIM(ADJUSTL(file5))

  OPEN(15,file=path22a5,status='old')
  DO j=1,ny
    READ(15,11)(trans(i,j),i=1,nx)
  END DO
  CLOSE(15)

!Multiply transmissivity field within the mining zones by random coefficient
  DO j=1,ny
    DO i=1,nx
      IF(imine(i,j).eq.1)THEN
        trans(i,j)=trans(i,j)*rnum(ifinished)
      ENDIF
    END DO
  END DO

!Output new transmissivity field
  path1f2a6=TRIM(path1)//"full/"//TRIM(ADJUSTL(file2a))//
  & "/"//TRIM(ADJUSTL(file6))

  OPEN(16,file=path1f2a6,status='unknown')
  DO j=1,ny
    WRITE(16,41)(trans(i,j),i=1,nx)
  END DO
  CLOSE(16)

END DO

!Format declarations
11 FORMAT(224e12.5)
```

Y.M.O. NOT A RECOMMENDATION

21 FORMAT(22413)
41 FORMAT(224e12.5)
5000 STOP
END

Appendix B: Partial Mining Conversion Code, PM.F

```
!Conversion program for partial mining case. This program reads two data sets,  
!Tupdate.mod and full_mining.dat. Tupdate.mod contains the calibrated t-fields  
!from Task 4. Partial_mining.dat is a digitized file consisting of a single integer  
!for each cell in the grid: 0 - inactive, 1 - mining zone, 2 - nonmining zone.  
!The transmissivities in the mining areas are then multiplied by a random number  
!between 1 and 1000 to simulate the random increase in transmissivity caused by  
!mining disturbance. The new t-field values are output to an ascii file for input  
!to MODFLOW. Two other parameter files are read, Good_runs.txt and mfr*.txt.  
!Good_runs.txt contains the list of calibrated T-fields from Task 4 and  
!mfr*.txt contains the random mining factors for each replicate. R* is either  
!R1, R2, or R3, depending on the replicate number.  
!Variable list:  
!dx,dy = cell dimension in the x and y directions  
!nx,ny = number of cells in the x and y directions  
!imine = input array of mining, non-mining, and inactive zones  
!trans = input array of calibrated t-field from Task 4  
!rnum = input variable of random mining multiplier  
!file1 = name of mining zone input file  
!file1a = name of replicate file  
!file2 = name of finished run file  
!file2a = name of finished run  
!file3 = name of random mining factor input file  
!file5 = name of t-field input file  
!file6 = name of modified t-field output file  
!path1 = name of local directory  
!path2 = name of remote t-field directory  
!path1f2a6 = path1 + "full" + file2a + file6  
!path22a5 = path2 + file2a + file5  
!5/7/03 - Thomas S Lowry !Modified 6/27/03, 8/12/03 - TSL  
  
PROGRAM PM_Main  
PARAMETER(dx=100,dy=100,nx=224,ny=307)  
INTEGER imine(nx,ny)  
REAL*8 trans(nx,ny),rnum(100)  
REAL no_min_hd(nx,ny),min_hd(nx,ny)  
  
CHARACTER*40 file1,file2,file2a,file3,file5,file6  
CHARACTER*12 fname,filz  
CHARACTER*65 path1,path2,path1f2a6,path22a5  
CHARACTER*3 realize  
CHARACTER*2 rep  
  
!Input file names  
DATA file1/"Part_mining.dat"/  
DATA file2/"Good_runs.txt"/  
DATA file5/"Tupdate.mod"/  
DATA file6/"CMine.mod"/  
DATA path2/"h/wipp/data/"/  
  
!Get replicate number  
READ(*,*)rep  
file3="mf"//rep//".txt"  
  
!Set base path  
path1="/home3/talowry/wipp/mining"//rep//"/"
```

```
!Open mining file and read mining zones
OPEN(11,file=TRIM(file1),status='old')
DO j=1,ny
  READ(11,*)(imine(i,j),i=1,nx)
END DO
CLOSE(11)

!Open file of finished t-field calibration runs
OPEN(12,file=TRIM(ADJUSTL(file2)),status='old')

!Read random mining factor
OPEN(13,file=file3,status='old')
READ(13,*)istop
DO i=1,istop
  READ(13,*)idumb,rnum(i)
END DO

!Read each finished t-field run, if end of file, go to end
DO ifinished=1,1000
  READ(12,'(a6)',END=5000)file2a

!Open calibrated t-field file and read in transmissivities
!Note: cell counting is based on MODFLOW grid, i.e. x-direction
!is left to right and y-direction is top to bottom.
path22a5=TRIM(ADJUSTL(path2))/TRIM(ADJUSTL(file2a))//"/"//
& TRIM(ADJUSTL(file5))
OPEN(15,file=path22a5,status='old')
DO j=1,ny
  READ(15,11)(trans(i,j),i=1,nx)
END DO
CLOSE(15)

!Multiply transmissivity field within the mining zones by random coefficient
DO j=1,ny
  DO i=1,nx
    IF(imine(i,j).eq.1)THEN
      trans(i,j)=trans(i,j)*rnum(ifinished)
    ENDIF
  END DO
END DO

!Output new transmissivity field
path1f2a6=TRIM(path1)//"partial/"//TRIM(ADJUSTL(file2a))//
& "/"//TRIM(ADJUSTL(file6))
OPEN(16,file=path1f2a6,status='unknown')
DO j=1,ny
  WRITE(16,41)(trans(i,j),i=1,nx)
END DO
CLOSE(16)

END DO

!Format declarations
11 FORMAT(224e12.5)
21 FORMAT(224i3)
41 FORMAT(224e12.5)
```


Appendix C: Grid Refinement Code, REFINE.F

```
! This program reads in calibrated t-field from Task 4 and
! refines the grid to 50x50m cell size. The new t-field is
! used as input for MODFLOW and subsequent input to SECOTP.
! Program assumes original grid size is 100x100m.

PARAMETER(nx=224,ny=307,nnx=448,nnny=614,dOld=100,dNew=50)
REAL tOld(nx,ny),tNew(nnx,nnny)

CHARACTER*40 file1,file2,file3,file4,file5
CHARACTER*12 fname,filz
CHARACTER*50 path1,path2,path3,path4,path5
CHARACTER*3 realize
CHARACTER*2 rep

DATA file1/"CMine.mod"/
DATA file2/"TNew.mod"/
DATA file3/"Good_runs.txt"/
DATA path1/"h/wipp/data/runs/"

!Get replicate number
READ(*,*)rep

!Set base path
path4="/home3/tslowry/wipp/mining/"//rep//"/"

!Open file of finished t-field calibration runs
OPEN(11,file=TRIM(ADJUSTL(file3)),status='old')

!Read each finished t-field run, if end of file, go to end
DO ifinished=1,1000
  READ(11,'(a6)',END=100)path2

!Extract realization number from directory naming convention
DO is=1,2
  IF(is.eq.1)THEN
    path3=TRIM(path4)//"full"//"/"
  ELSE
    path3=TRIM(path4)//"partial"//"/"
  ENDIF

!Goto directory with finished t-field
OPEN(12,file=TRIM(path3)//TRIM(ADJUSTL(path2))//"/"//
  & TRIM(ADJUSTL(file1)),status='old')

!Read in calibrated t-field
DO j=1,ny
  READ(12,'(224e12.5)')(tOld(i,j),i=1,nnx)
END DO
CLOSE(12)

!Transfer old values to new grid
DO jn=1,nnny
  DO in=1,nnx
    io=1+INT((in-1)*dNew/dOld)
    jo=1+INT((jn-1)*dNew/dOld)
```



```
        tNew(in,jn)=tOld(io,jo)
      END DO
    END DO

!Output to new file
      OPEN(13,file=TRIM(path3)//TRIM(ADJUSTL(path2))//
&      "///TRIM(ADJUSTL(file2)),status='unknown')
      DO jn=1,nny
        WRITE(13,'(448e12.5)')(tNew(in,jn),in=1,nxx)
      END DO
      CLOSE(13)
    END DO
  END DO
100 STOP
END
```

ALL INFORMATION CONTAINED
HEREIN IS UNCLASSIFIED

EXCEPT WHERE SHOWN
OTHERWISE INFORMATION ONLY

Appendix D: Binary to ASCII Conversion: BA.F

!Program to convert MODFLOW flow budget binary file to !ASCII format.

```
PROGRAM AsciiBud
PARAMETER(nx=448,ny=614,ndbmx=nx*ny)

REAL qx(nx,ny),qy(nx,ny)
REAL xdumb
CHARACTER*40 file1,file2,file2a,file3,mine
CHARACTER*68 path1,path2,path1f2a1,path1f2a3
CHARACTER*16 text
CHARACTER*2 rep(3)
INTEGER kstp,kper,ncol,nrow,nlay,nlist,imeth
REAL deltax,pertim,totim

!Input file names
DATA file1/"steady50x50.bud"/
DATA file2/"Good_runs.txt"/
DATA file3/"steady50x50_ascii.dat"/
DATA path2/"h/wipp/data"/
DATA rep/"R1","R2","R3"/

DO ir=1,3

!Assign base path
path1="/home3/tslowry/wipp/mining/"//rep(ir)//"

!Open file of finished t-field calibration runs
OPEN(2,file=TRIM(ADJUSTL(file2)),status='old')

!Read each finished t-field run, if end of file, go to end
DO ifinished=1,1000
  READ(2,'(a6)',END=5000)file2a
  mine="full/"
  DO imine=1,2
    IF(imine.eq.2)mine="partial/"
!Read in cell-by-cell flow file
  path1f2a1=TRIM(path1)//TRIM(ADJUSTL(mine))//
  & TRIM(ADJUSTL(file2a))//
  & "/"//TRIM(ADJUSTL(file1))

!
! Read volumetric flow field in m3/sec from MODFLOW *.ccf file.
! Flow across right face is the flow between cell i,j and i+1,j
! Flow across front face is the flow between cell i,j and i,j-1
! using column (i), row (j), counting in this model
!
  OPEN(13,file=path1f2a1,status='old',form='unformatted')
  DO i=1,3
20    READ(13,END=25)kstp,kper,text,ncol,nrow,nlay
    READ(13)itemp,deltax,pertim,totim
    IF(TRIM(ADJUSTL(text)).eq."CONSTANT HEAD")THEN
      READ(13)nlist
      DO in=1,nlist
        READ(13)xdumb
      END DO
    END DO
  END DO
```

```
ELSEIF(TRIM(ADJUSTL(text)).eq."FLOW FRONT FACE")THEN
  READ(13)qy
ELSEIF(TRIM(ADJUSTL(text)).eq."FLOW RIGHT FACE ")THEN
  READ(13)qx
ENDIF
END DO
!GOTO 20
25      CLOSE(13)

! Open file for ASCII output
path1f2a3=TRIM(path1)//TRIM(ADJUSTL(mine))//
&      TRIM(ADJUSTL(file2a))//
&      "/"//TRIM(ADJUSTL(file3))

OPEN(15,file=path1f2a3,status='unknown')

DO j=1,ny
  WRITE(15,150)(qx(i,j),i=1,nx)
END DO

WRITE(15,*)

DO j=1,ny
  WRITE(15,150)(qy(i,j),i=1,nx)
END DO
CLOSE(15)

END DO
END DO
5000 CONTINUE
CLOSE(2)
END DO

150 FORMAT(448e16.8)

STOP
END
```

Appendix E: Particle Tracking Post-processing, PTOUT.F

!The program reads in each DTRKMF output file and combines the results
!into one file for post processing in EXCEL. Output is two separate files
!one for full mining case and the other the partial mining case.
!6/16/03 - Thomas S Lowry

```
PROGRAM PTOUT_Main
PARAMETER(runs=200,times=1000)
REAL*8 dtime(times,runs),xd(times,runs),yd(times,runs)
INTEGER etime(runs),xrc
CHARACTER*36 path1
CHARACTER*18 finished(runs),file1
CHARACTER*6 fin
CHARACTER*7 mine
CHARACTER*2 rep(3)

DATA file1/"Replicate.txt"/
DATA rep/"R1","R2","R3"/

DO ir=1,3

!Set base path
path1="/home3/tslowry/wipp/mining/"//rep(ir)//"/"//ptout/"

dtime=-999
xd=-888
yd=-777
xrc=0

DO ip=1,2
  IF(ip.eq.1)THEN
    mine="full"
  ELSE
    mine="partial"
  ENDIF
  OPEN(1,FILE='Good_runs.txt',STATUS='OLD')
  DO j=1,runs
    READ(1,*,END=100)fin
    xrc=xrc+1
    finished(xrc)=fin//"-"/TRIM(ADJUSTL(mine))//".out"
    OPEN(3,FILE=path1//TRIM(ADJUSTL(finished(xrc))),
      & STATUS='OLD')
    READ(3,*)temp0,itime
    DO i=1,itime
      READ(3,*,END=200)dtime(i,xrc),temp1,temp2,
      & xd(i,xrc),yd(i,xrc)
    END DO
  CONTINUE
  CLOSE(3)
END DO
200 CONTINUE
END DO
100 CONTINUE
CLOSE(1)
END DO

OPEN(2,FILE=path1//ptout.out,STATUS='UNKNOWN')
OPEN(13,FILE=path1//times.out,STATUS='UNKNOWN')
```

```
DO ip=1,2
  WRITE(2,20)(finished(j),j=(ip-1)*xrc/2+1,xrc/2+(ip-1)*xrc/2)
  DO i=1,times
    WRITE(2,21)(dtime(i,j),xd(i,j),yd(i,j),
      &         j=(ip-1)*xrc/2+1,xrc/2+(ip-1)*xrc/2)
    END DO
    WRITE(2,*)
  END DO

DO j=1,xrc
  DO i=1,times
    IF(dtime(i,j).lt.0)THEN
      WRITE(13,33)finished(j),dtime(i-1,j)
      EXIT
    ENDIF
  END DO
END DO

20 FORMAT(100a48)
21 FORMAT(100(3f16.6))
33 FORMAT(a13,f16.5)

5000 STOP
END
```

Appendix F: Particle Tracking Post-processing, PTPLOT.F

!The program reads in each DTRKMF output file and combines the results
!into one file for post processing in EXCEL. Output is two separate files
!one for full mining case and the other the partial mining case.
!6/16/03 - Thomas S Lowry

```
PROGRAM PTPLOT_Main
PARAMETER(runs=200,times=1000)
REAL*8 xd(times,runs),yd(times,runs)
INTEGER itime,xrc
CHARACTER*36 path1
CHARACTER*18 finished(runs)
CHARACTER*6 fin
CHARACTER*7 mine
CHARACTER*2 rep(3)

DATA rep/"R1","R2","R3"/

DO ir=1,3
!Set base path
  path1="/home3/tslowry/wipp/mining/"//rep(ir)//"/"//ptout/"

  dtime=-999
  xd=-601700
  yd=3697200
  xrc=0

  DO ip=1,2
    IF(ip.eq.1)THEN
      mine="full"
    ELSE
      mine="partial"
    ENDIF
    OPEN(1,FILE='Good_runs.txt',STATUS='OLD')
    DO j=1,runs
      READ(1,*,END=100)fin
      xrc=xrc+1
      finished(xrc)=fin
      OPEN(3,FILE=path1//fin//"-"/TRIM(ADJUSTL(mine))//
        & ".out",STATUS='OLD')
      READ(3,*)temp0,itime
      DO i=1,itime
        READ(3,*,END=200)temp0,temp1,temp2.
        & xd(i,xrc),yd(i,xrc)
      END DO
      CONTINUE
      CLOSE(3)
    END DO
    CONTINUE
    CLOSE(1)
  END DO

  OPEN(2,FILE=path1//plot.out,STATUS='UNKNOWN')

  DO ip=1,2
    WRITE(2,20)(finished(j),j=(ip-1)*xrc/2+1,xrc/2+(ip-1)*xrc/2)
```

INFORMATION ONLY

```
      DO i=1,times
        WRITE(2,21)(xd(i,j)+601700,3597200-yd(i,j),
&          j=(ip-1)*xrc/2+1,xrc/2+(ip-1)*xrc/2)
        END DO
      END DO
      END DO
20  FORMAT(100a32)
21  FORMAT(100(2f16.3))

5000 STOP
      END
```

Y:\MO MGT\AP-088-711

INFORMATION ONLY

Appendix G: Linux Shell Script: MINING.SH

```
#For Task 5 of AP-088 and Tasks 2 and 3 of AP-100
#THISDIR is equal to: '/home3/tslowry/wipp/mining'
THISDIR='pwd'
SIDIR=$THISDIR/100x100
S5DIR=$THISDIR/50x50
MODDIR=/home2/wipp/data
SCENARIO="full partial"
REPLICATE='cat Replicate.txt'
FINISHED='cat Good_runs.txt'

#Loop through each replicate
for rep in $REPLICATE
do
    cd ./$rep

#Loop through the full and partial mining scenarios
    for scn in $SCENARIO
    do
        cd ./$scn
        echo 'Writing files to '$rep/$scn' directory.'

#Loop through each realization
        for Run in $FINISHED
        do

#Make directory and copy steady-state files
            mkdir ./Run
            cd ./Run
            cp $SIDIR/culebra.top ./fort.33
            cp $SIDIR/culebra.bot ./fort.34
            cd ..
        done
        cd $THISDIR/$rep
    done

    cd $THISDIR

    echo 'Executing fm'
    echo $rep | fm
    echo 'Executing pm'
    echo $rep | pm
    echo 'Executing refine'
    echo $rep | refine

    cd ./$rep

#Loop through full and partial mining scenarios and
#run MODFLOW and DTRKMF for AP-088 and MODFLOW for AP-100

    for scn in $SCENARIO
    do
        cd ./$scn

        for Run in $FINISHED
        do
```



```
cd ./Run
mf2k $$S1DIR/steady.nam
echo 'Finished with MF2K 100x100 in' $rep/$scn/$Run
dtrkmf < $$S1DIR/dtrkmf.in
echo 'Finished with DTRKMF in' $rep/$scn/$Run
rm fort.33
rm fort.34
mf2k $$S5DIR/steady.nam
echo 'Finished with MF2K 50x50 in' $rep/$scn/$Run
rm *.hed
rm *.lst
cd ..
done

cd $THISDIR/$rep
done
cd $THISDIR
done

cd $THISDIR

#Move dtrkmf output files to common directory
sh post.sh

#Combine dtrkmf output to two separate files (full and part)
echo 'Running ptout'
ptout

#Put all X-Y Coordinate pairs into one file for plotting purposes
echo 'Running ptplot'
ptplot

#Create ASCII budget file from MODFLOW binary output
echo 'Executing ASCII conversion program: ba'
ba

#Move all ASCII budget files to one directory for easy ftp
sh post-flow.sh

#Finished!
echo 'Finished!'
```

2/1/70 10:17 AM

INFORMATION ONLY

Appendix H: Linux Shell Script: POST.SH

```
#This script is to collect the DTRKMF output for each
#realization into a single directory to allow for easier
#access when post-processing. Each replicate directory
#will contain a sub-directory called 'ptout' that holds
#all the files.
#THISDIR = '/home3/tslowry/wipp/mining'

THISDIR='pwd'
SCENARIO="full partial"
REPLICATE='cat Replicate.txt'
FINISHED='cat Good_runs.txt'

#Loop through each replicate
for rep in $REPLICATE
do

#Make particle tracking output directory
mkdir ./$rep/ptout

#Loop through the full and partial mining scenarios
for scn in $SCENARIO
do

#Loop through each realization, get each particle tracking output,
#and copy to output directory
for Run in $FINISHED
do
    cp ./$rep/$scn/$Run/dtrk.out ./$rep/ptout/$Run-$scn.out
done
done
done
```

Appendix I: Linux Shell Script: POST-FLOW.SH

```
#This script collects the ASCII flow budget file
#produced by ba.f within each realization directory
#and places them in a single directory called 'aff'.

THISDIR='pwd'
SCENARIO="f p"
REPLICATE='cat Replicate.txt'
FINISHED='cat Good_runs.txt'

for rep in $REPLICATE
do

#Make ASCII flow-file output directory
mkdir ./$rep/aff

#Loop through the full and partial mining scenarios
for scn in $SCENARIO
do

#Designate directory
if test $scn = p
then
smdir=partial
else
smdir=full
fi

#Loop through each realization
for Run in $FINISHED
do

#Get each particle tracking output and copy to output directory
cp ./$rep/$smdir/$Run/steady50x50_ascii.dat ./$rep/aff/$Run$scn$rep.out
rm ./$rep/$smdir/$Run/steady50x50_ascii.dat
done
done
done
```

CLASSIFICATION

INFORMATION ONLY

Appendix J: Qualified Runs and Random Mining Factors

Qualified runs and random mining factors for each replicate.

Run #	R1	R2	R3
d01r02	905.50	32.86	13.54
d01r04	508.40	345.10	202.20
d01r07	340.30	996.50	936.30
d01r10	615.20	828.20	391.80
d02r02	575.30	579.30	306.80
d03r01	104.00	760.50	955.80
d03r03	94.06	514.90	77.79
d03r06	913.30	187.60	238.40
d03r07	630.50	567.10	725.20
d03r08	208.90	475.90	85.67
d03r09	769.30	750.00	647.80
d04r01	130.20	630.30	478.70
d04r02	351.90	453.30	996.70
d04r03	46.87	310.90	123.90
d04r04	194.60	487.90	217.30
d04r05	806.90	923.80	138.30
d04r06	264.40	584.00	835.30
d04r07	931.50	733.90	802.00
d04r08	897.90	51.08	96.80
d04r10	32.56	256.50	34.02
d05r03	394.10	108.30	159.00
d05r07	998.20	535.90	145.50
d06r02	790.00	679.40	826.70
d06r03	384.10	171.20	261.20
d06r04	258.50	860.00	293.90
d06r05	432.50	754.10	257.60
d06r06	10.02	653.20	172.50
d06r07	514.10	221.50	915.60
d06r10	282.90	70.11	861.40
d07r01	927.30	694.20	625.20
d07r02	691.30	864.90	737.80
d07r05	738.40	775.30	241.60
d07r06	450.20	591.70	548.70
d07r07	609.60	447.20	841.00
d07r08	557.70	942.30	349.00
d07r09	538.60	98.94	285.00
d07r10	713.60	379.60	187.30
d08r01	849.30	408.40	194.00
d08r02	569.70	989.10	893.90
d08r03	419.50	43.16	356.30
d08r04	160.00	834.00	857.00
d08r05	971.90	881.10	671.60
d08r06	118.80	558.90	743.20
d08r07	741.30	130.20	706.70
d09r02	729.70	497.00	429.30
d09r03	483.00	197.30	168.20
d09r04	580.60	661.30	766.40
d09r05	228.50	240.90	481.90
d09r06	474.10	383.50	449.10
d09r07	887.20	952.10	503.30

d09r08	66.07	339.80	327.30
d09r09	375.70	806.30	374.20
d09r10	521.10	906.90	24.83
d10r02	181.60	274.60	651.90
d10r03	298.50	796.60	816.70
d10r04	705.30	364.70	518.20
d10r06	84.20	819.40	690.80
d10r07	627.30	728.60	551.20
d10r08	403.20	414.80	670.30
d10r09	464.20	649.90	885.40
d10r10	821.40	607.80	925.70
d11r01	307.60	895.10	492.90
d11r02	236.50	918.30	364.50
d11r06	249.90	159.70	5.43
d11r07	543.50	86.78	966.70
d11r08	18.75	16.92	973.80
d11r09	215.40	618.30	576.30
d11r10	73.60	168.90	403.20
d12r01	317.40	683.30	756.20
d12r02	958.60	204.90	598.10
d12r03	686.00	322.00	333.80
d12r05	860.70	637.50	589.70
d12r06	363.80	359.00	56.06
d12r07	660.40	434.90	463.10
d12r08	940.20	708.20	312.10
d12r09	132.50	464.10	794.60
d13r01	983.00	971.30	901.70
d13r02	672.80	144.50	224.80
d13r03	643.20	849.00	415.20
d13r05	425.80	118.60	688.00
d13r06	961.10	785.90	385.40
d13r07	346.10	282.90	711.40
d13r08	838.60	78.26	64.98
d13r09	491.00	8.68	458.00
d21r01	755.40	307.30	632.40
d21r02	172.60	396.20	614.80
d21r03	591.50	422.30	45.61
d21r04	322.70	715.50	276.80
d21r05	855.70	870.90	105.80
d21r06	272.00	501.20	984.40
d21r07	652.50	296.70	940.20
d21r10	790.50	212.70	562.50
d22r02	163.20	527.50	870.80
d22r03	812.70	264.30	534.50
d22r04	144.70	140.70	526.30
d22r06	26.04	962.70	111.70
d22r07	870.30	548.10	609.10
d22r08	773.60	235.30	771.70
d22r09	53.04	937.70	784.10
d22r10	460.40	24.35	434.60

